Journal of Statistical Physics, Vol. 54, Nos. 3/4, 1989

From Equilibrium Spin Models to Probabilistic Cellular Automata

Antoine Georges[1] and Pierre Le Doussal[1,2]

Received December 10, 1987; final October 10, 1988

The general equivalence between D-dimensional probabilistic cellular automata (PCA) and $(D+1)$-dimensional equilibrium spin models satisfying a "disorder condition" is first described in a pedagogical way and then used to analyze the phase diagrams, the critical behavior, and the universality classes of some automata. Diagrammatic representations of time-dependent correlation functions of PCA are introduced. Two important classes of PCA are singled out for which these correlation functions simplify: (1) "Quasi-Hamiltonian" automata, which have a current-carrying steady state, and for which some correlation functions are those of a D-dimensional static model. PCA satisfying the detailed balance condition appear as a particular case of these rules for which the current vanishes. (2) "Linear" (and more generally "affine") PCA for which the diagrammatics reduces to a random walk problem closely related to $(D+1)$-dimensional directed SAWs: both problems display a critical behavior with mean-field exponents in any dimension. The correlation length and effective velocity of propagation of excitations can be calculated for affine PCA, as is shown on an explicit $D=1$ example. We conclude with some remarks on nonlinear PCA, for which the diagrammatics is related to reaction-diffusion processes, and which belong in some cases to the universality class of Reggeon field theory.

KEY WORDS: Probabilistic cellular automata; lattice spin models; disorder solutions; phase transitions.

[1] Laboratoire de Physique Théorique de l'École Normale Supérieure (Laboratoire propre du Centre National de la Recherche Scientifique, associé à l'École Normale Supérieure et à l'Université de Paris-Sud), France.

[2] Present address: Sloane Laboratory, Physics Department, Yale University, New Haven, Connecticut.

0022-4715/89/0200-1011$06.00/0

INTRODUCTION

This paper is devoted to the link between probabilistic cellular automata (PCA) and the so-called "disorder solutions" of anisotropic lattice spin models. A PCA is an array of discrete variables which are simultaneously updated in discrete time steps according to some local preassigned probabilistic rules.[1–3] The probability measure over space-time histories of an arbitrary D-dimensional PCA can be seen as the Boltzmann weight of a $(D+1)$-dimensional *equilibrium* spin model. This equilibrium model is anisotropic, and its coupling constants can be calculated from the parameters specifying the evolution rule of the PCA. As a consequence, these coupling constants are not independent, but are linked by some relationship which, in the context of equilibrium spin models, is usually known as a "disorder condition" (a name used mainly for historical reasons[4]).

The mapping of a PCA onto an equilibrium spin model is not new: it was discovered in the study of crystal growth models[5–8] (an old-fashioned name for some particular PCA) and has been used since by some authors.[9–13] A recent article by Rujan[12] and—we hope—the present paper are complementary attempts to use this general equivalence between PCA and "disorder solutions" of spin models in order to study dynamical properties of PCA, a question which has not yet been systematically investigated.

This paper has two main purposes. The first one is to present this equivalence in a unified and self-contained manner: this is the aim of Section 1 (Sections 1.1–1.5). These sections have, to a large extent, the character of a review (which, however, intends to give an original presentation and does not mean to be exhaustive). The second one, to which Section 1.6 and Section 2 are devoted, is to show how this equivalence can be used in order to study the dynamical behavior of PCA, with particular emphasis on their phase transitions and universality classes. For the sake of convenience, *the detailed organization and contents of these two parts can be found at their beginning.*

Having presented the general approach of the paper, it can be useful, due to its length, to give at this point a brief summary of the main new results that it contains. The general equivalence between PCA and "disorder solutions" of equilibrium spin models is described in Sections 1.1–1.2, and applied to the most general one-dimensional nearest-neighbor one-step PCA in Section 1.3 (several other examples are given in Sections 1.4–1.5). We discuss in Section 1.6 a particular class of PCA rules (called "quasi-Hamiltonian" ones) which display a current-carrying steady state and for which some correlation functions are those of a D-dimensional static

model. In Section 2, diagrammatics and decimation techniques are introduced for the calculation of time-dependent correlation functions (which amounts to a static problem in the associated equilibrium spin model). This makes it possible to single out and to study in detail (Sections 2.1–2.3) the class of "affine" (and "linear") rules [22,12,25] for which the calculation of correlation functions reduces to a random walk problem (they are equivalent in some particular cases to "voters models"; (e.g., ref. 63). This is illustrated by a specific example in Section 2.2, for which the relaxation-time and two-point correlation functions are explicitly calculated, as well as the "effective velocity of sound" characterizing the diffusion of an initial excitation. Phase transitions of "linear" rules are studied in Section 2.3 and their universality class is shown to be related to the problem of directed self-avoiding walks and to displaying mean-field exponents in any dimensionality. These techniques also allow one to extend dynamical and critical properties of PCA satisfying the detailed balance property to the more general case of "quasi-Hamiltonian" rules (Section 2.4) and to analyze in a simple and unified way the phase transitions of some nonlinear rules (Section 2.5).

1. CELLULAR AUTOMATA AND SPIN MODELS

In this part, we describe the mapping between a D-dimensional PCA and a $(D+1)$-dimensional equilibrium spin model. For pedagogical reasons, we first deal with an explicit example, which is detailed in Section 1.1. We then turn to the general scheme (Section 1.2) and show, in particular, that the criterion introduced by Jaekel and Maillard[14] for "disorder solutions" of spin models identifies with the normalization of probability in the PCA framework. A number of explicit examples of 1D and 2D PCA and of their associated equilibrium models are given in Sections 1.3–1.5 (including, in particular, the most general nearest neighbor 1D PCA). After a summary of elementary symmetry properties of PCA rules, we discuss in Section 1.6 the detailed balance principle. Finally, in connection with the possibility of defining an asymptotic measure over configurations, we point out the existence of an important class of rules, which we call "quasi-Hamiltonian."

1.1. A Pedagogical Example

The example we shall now deal with has been considered in particular cases by Verhagen[15] and Enting[7] and, more recently, by Domany and Kinzel[10] for its relation with directed percolation. Consider a linear chain of sites (Fig. 1a), each supporting a binary variable $S_i = +1, -1$. Starting

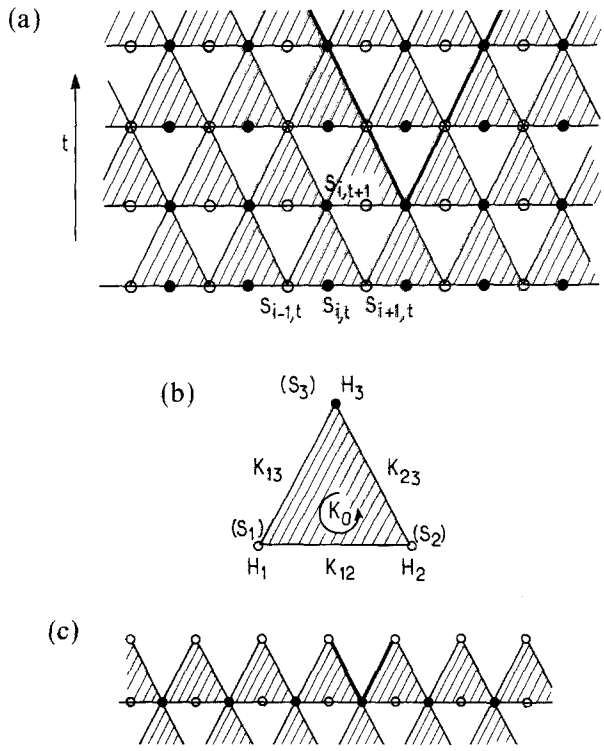

Fig. 1. (a) The space-time triangular lattice generated by the evolution of the PCA described in the text. (b) Coupling constants between the spins of an elementary cell of the lattice. (c) Boundary conditions used for the calculation of the partition function.

from a given configuration, the chain evolves in discrete time steps: at even (resp. odd) time steps, the even-indexed (resp. odd-indexed) spins can change their states simultaneously, according to preassigned probabilistic rules. These rules are chosen to depend only on the states of the two nearest neighbors, and are thus characterized by four conditional probabilities $P(S_{i,t+1}/S_{i-1,t}, S_{i+1,t})$:

$$x = P(1/-1, -1), \quad z = P(1/1, 1), \quad y_1 = P(1/-1, 1), \quad y_2 = P(1/1, -1) \tag{1.1}$$

which $0 \leqslant x,\ y_i,\ z \leqslant 1$ and $P(-S_3/S_1, S_2) = 1 - P(S_3/S_1, S_2)$. This can be summarized in the following expression for the conditional probability:

$$P(S_3/S_1, S_2) = 1/2 \cdot [1 + S_3(V + T_1 S_2 + T_2 S_1 + U S_1 S_2)] \tag{1.2}$$

where the parameters T_1, U, V are related to x, y_1, y_2, z through the relations

$$\begin{aligned} T_1 &= 1/2 \cdot (z - x + y_1 - y_2), \qquad T_2 = 1/2 \cdot (z - x + y_2 - y_1) \\ U &= 1/2 \cdot (z + x - y_1 - y_2), \qquad V = 1/2 \cdot (z + x + y_1 + y_2 - 2) \end{aligned} \tag{1.3}$$

Consider now a given "history" of the PCA, that is, a set of successive states $\{S_{i,t}\}$; due to the Markovian nature of the evolution, the probability of this history reads

$$P[\{S_{i,t}\}] = \prod_t \prod_i P(S_{i,t+1} \mid S_{i-1,t}, S_{i+1,t}) \tag{1.4}$$

This suggests the rewriting of $P(S_3/S_1, S_2)$ in an exponential form, well suited to express products like (1.4). This can be done in a straightforward way:

$$\begin{aligned} P(S_3/S_1, S_2) = \lambda^{-1} \exp(&H_1 S_1 + H_2 S_2 + H_3 S_3 + K_{12} S_1 S_2 + K_{23} S_2 S_3 \\ &+ K_{13} S_1 S_3 + K_0 S_1 S_2 S_3) \end{aligned} \tag{1.5}$$

where the expression of λ, H_i, K_{ij}, and K_0 in terms of x, y_1, y_2, and z is given in Eqs. (A.2)–(A.3) of Appendix A. The trick is now to view the successive states of the chain as the successive rows of a two-dimensional triangular lattice, as depicted in Fig. 1a (the time direction playing the role of the second dimension). The probability of the "history" $\{S_{i,t}\}$ becomes

$$P(\{S_{i,t}\}) = 1/Z \exp[-\beta H(S_{i,t})] \tag{1.6}$$

where H is the Hamiltonian of a spin model defined on this triangular lattice and involving magnetic fields, two-site and three-site interactions, in each elementary plaquette (hatched triangle depicted in Fig. 1b), namely

$$\begin{aligned} -\beta H = &(H_1 + H_2 + H_3) \sum_i S_i \\ &+ \sum_{\triangle} (K_{12} S_1 S_2 + K_{23} S_2 S_3 + K_{13} S_1 S_3 + K_0 S_1 S_2 S_3) \end{aligned} \tag{1.7}$$

Nature of the Equilibrium Model. We have thus mapped the time development of a 1D PCA onto equilibrium properties of a 2D spin model. However, *this spin model is a very peculiar one*: it is anisotropic, and its coupling constants (H_i, K_{ij}, K_0) are not all independent but are linked together by some relationship. This is *a priori* obvious, since these seven coupling constants are in fact functions only of the four independent

parameters x, y_1, y_2, z. Stated differently, the Boltzmann weight $W(S_3, S_2, S_1)$ of an elementary triangle is related to the conditional probability through $W = \lambda P(S_3/S_2, S_1)$ and thus satisfies the normalization condition

$$\sum_{S_3 = \pm 1} W(S_3, S_2, S_1) = \lambda \tag{1.8}$$

where λ depends on the coupling constants only and not on the spins S_1 and S_2. This enforces directly some relationships between H_i, K_{ij}, and K_0, of which Eq. (A.3) of Appendix A can be seen as a parametrization. Note that the equilibrium spin model is in fact defined by five coupling constants (and not seven), since the total field on each lattice site is the symmetric combination $H_1 + H_2 + H_3 = h$; Eq. (1.8) thus defines a codimension-1 variety in the phase diagram parametrized by (h, K_{ij}, K_0) (called, as we shall see, a "disorder variety"). To be fully explicit, let us quote the relationship defining this variety in the simplified case where K_0 is taken to be zero (that is, for the anisotropic triangular Ising model with a field). One finds[14,15]

$$\begin{aligned} &t_1 t_2 t_3 (1+t_1)^2 (1+t_2)^2 (1-t_3)^2 (1-a)^2 \\ &\quad + 4(1 + t_1 t_2 t_3)(t_1 + t_2 t_3)(t_2 + t_1 t_3)(t_3 + t_1 t_2) a = 0 \\ &\lambda = 2[(1-t_3^2)(1-t_1^2)^{-1}(1-t_2^2)^{-1}(-t_1 t_2 t_3^{-1})]^{1/2} \end{aligned} \tag{1.9}$$

where $a = \exp 2(H_1 + H_2 + H_3)$, $t_1 = \tanh(K_{23})$, etc.

The most remarkable feature of the model (1.7) constrained by Eq. (1.8) is that its partition function *can be calculated exactly*. Indeed, summing (1.4) over all possible "histories" leads to

$$1 = \sum_{\{S_{i,t}\}} P[\{S_{i,t}\}] = \sum_{\{S_i\}} \prod_{\blacktriangle} P(S_3 | S_1, S_2) = \lambda^{-N_p} \sum_{\{S\}} \prod_{\blacktriangle} W \tag{1.10}$$

where N_p is the number of hatched triangles in the lattice. We thus conclude that the partition function simple reads

$$Z = \lambda^{N_p} \tag{1.11}$$

We have in fact been lax about the boundary conditions to be chosen: let us give now a more careful derivation, due to Jaekel and Maillard.[14] It is based on a "decimation" method which will be useful in Section 2 for the calculation of correlation functions. The trick is to impose the particular boundary conditions depicted to Fig. 1c on the upper layer of the 2D lattice: on this layer, all K_{12} interactions are missing. One can now sum over

the spins of this layer: thanks to condition (1.8), the same boundary conditions are recovered for the next layer, and each triangular plaquette simply contributes a factor λ to the partition function. The process can be repeated recursively, leading to (1.11) for the whole lattice.[3] Thus, the local condition (1.8) results in a decoupling of the spin degrees of freedom and in an effective reduction of dimensionality for the spin system. From the point of view of anisotropic equilibrium spin models, this remarkable phenomenon occurs whenever the coupling constants of the most general Ising model of the form (1.7) satisfy the relationship (1.8), i.e., on a particular subspace of the phase diagram. This is generally called a *disorder solution*, and condition (1.8) has indeed been proposed as a general rule to find disorder solutions of spin models.[14] This term can be traced back to the work of Stephenson[4] and stems from the fact that in some cases the correlation length is indeed minimum on the "disorder subspace" as a result of the local decoupling phenomenon.[4,17] Note, finally, that expression (1.11) for the partition function restricted to the disorder subspace is always a simple algebraic expression of the coupling constants [as can be seen on the example of (1.9)] and is therefore *free of any singularity*. As will be made clear in the following, this *does not mean* that no intersection can occur with the critical variety of the spin model.

1.2. General Scheme

It should be clear already that the example detailed above can be easily generalized to an arbitrary D-dimensional PCA. The general idea is to consider the successive states of the D-dimensional array as the successive layers of a $(D+1)$-dimensional lattice, the last dimension being the time. The Markovian and local nature of the evolution rule allows one to define a local Hamiltonian on this $(D+1)$-dimensional lattice such that the probability of a given "history" $\{S_{i,t}\}$ is equal to the thermodynamic weight of the configuration $\{S_{i,t}\}$ in the equilibrium model. This Hamiltonian involves in general, in each elementary cell, multispin coupling constants and fields, which are functions of the original conditional probabilities, and are thus linked by some relationship (through normalization of probability). Thus, the associated $(D+1)$-dimensional model is restricted to the "disorder variety" of its phase diagram. This general equivalence is summarized in Table I, where the correspondence between some quantities of interest is given.

It should be emphasized that a dynamical quantity for the PCA (such

[3] The Perron–Fröbenius theorem ensures that (1.11) is, indeed, the partition function of the model, despite the unusual boundary conditions chosen (see also ref. 16).

Table I. Equivalence between a D-Dimensional PCA and a $(D+1)$-Dimensional Spin Model Satisfying a "Disorder Condition"

D-Dimensional PCA	$(D+1)$-Dimensional spin model
Space-time "history" $\{S_{i,t}\}$	Spin configuration $\{S_{i,t}\}$
Local conditional probability $P(\{S'_{t+1}\}/\{S_t\})$	Normalized local Boltzmann weight $(1/\lambda)\, W(\{S'\}, \{S\})$
Normalization condition: $\sum_{\{S'\}} P(\{S'\}/\{S\}) = 1$	"Disorder condition" on coupling constants: $\sum_{\{S'\}} W(\{S'\}, \{S\}) = \lambda$, independant of S
Evolution operator	Row-to-row transfer matrix
Initial configuration	Boundary condition
Probability of a history: $P(\{S_{i,t}\})$	Thermodynamic weight: $1/Z \exp[-\beta H(S_{i,t})]$
$\langle \cdots \rangle$: Average over histories	Thermodynamic average
Dynamical correlation function: $\langle S_{i,t} S_{j,t}, \ldots \rangle_P$	Correlation function: $\langle S_{i,t} S_{j,t}, \ldots \rangle_H$
Transient phenomena	Surface effects
Deterministic limits	Different zero-temperature limits
Deterministic "histories"	Ground states

as a correlation function) corresponds to a bulk thermodynamic average in the associated spin model only when averaged over all possible "histories." As noted in ref. 12, transient phenomena in the PCA for a given initial condition correspond to surface effects in the spin model with fixed boundary conditions.

The deterministic limits of the PCA (where all conditional probabilities are taken to be zero or one) are of particular interest.[2,3] In these limits, all coupling constants of the spin model go to $+\infty$ or $-\infty$ [see Eq. (A.3)]. The different deterministic limits are thus associated with the different possible ways of taking the zero-temperature limit of the spin model while preserving relation (1.8) between coupling constants. Each particular time development of a deterministic CA corresponds to a different ground state of the equilibrium spin model with a given boundary condition.[10]

The general scheme described in this section can be adapted to a variety of situations which cannot all be reviewed here.[12,14,18] We will simply given some examples in the next three sections which each displays some features at variance with the example of Section 1.1.

It is worth mentioning that a D-dimensional PCA can also be seen as a quantum problem (spin model) in D dimensions: this is sketched in Appendix B.

1.3. The Most General Nearest Neighbor, Markovian, 1D PCA

The most familiar picture of a 1D PCA[1,3] is the case of binary spins $S_{i,t}$ on a line, with a simultaneous Markovian evolution characterized by the eight conditional probabilities $P(S_{i,t+1}/S_{i-1,t}, S_{i,t}, S_{i+1,t})$:

$$\begin{aligned} z &= P(1/1, 1, 1) & x &= P(1/-1, -1,, -1) \\ y_1 &= P(1/-1, 1, 1) & v_1 &= P(1/1, -1, -1) \\ y_0 &= P(1/1, -1, 1) & v_0 &= P(1/-1, 1, -1) \\ y_2 &= P(1/1, 1, -1) & v_2 &= P(1/-1, -1, 1) \end{aligned} \tag{1.12}$$

Thus, the state of a spin at time $t+1$ depends not only on its nearest neighbors at time t, but also on itself. The 2D lattice generated by the time evolution[12] is depicted in Fig. 2a: its elementary cell is the hatched triangle containing four sites. However, because of the simultaneous evolution of all sites, each of these cells has an overlap with two others. When no particular restriction is imposed on the conditional probability,

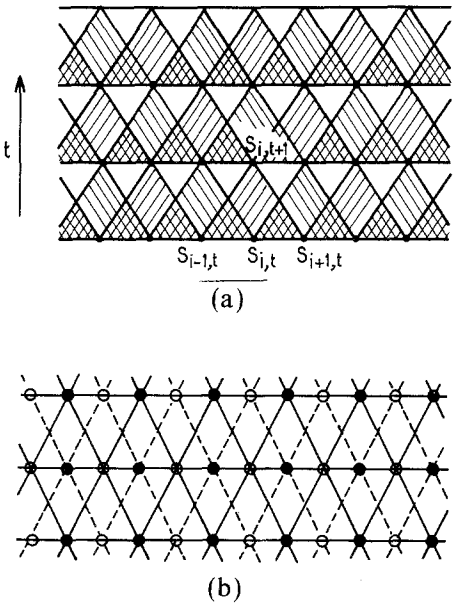

Fig. 2. (a) The space-time lattice associated with the general nearest-neighbor 1D PCA. Notice the overlapping cells. (b) Decoupling between the two sublattices in the "peripheral" case.

the Boltzmann weight $W(S_0/S_1, S_2, S_3)$ of an elementary cell involves all possible interactions among the four spins. The explicit expressions of these coupling constants in terms of the conditional probabilities are given in Eq. (A.11) of Appendix A. (In fact, due to the overlap between plaquettes, only 11 coupling constants are necessary to define this 2D spin model, which are linked by three "disorder conditions" through the normalization of P).

From the existence of three- and four-spin interactions as well as next-nearest neighbor interactions—some of which are negative—one may expect a very complicated phase diagram involving a variety of phases, as is the case, for example, for ANNNI models.[19] The same complexity is present in the structure of the ground states of the model, which are associated with one of the $2^8 = 256$ deterministic limits of the PCA (some of which are chaotic).[2,3] It is convenient to characterize these limits by their rule number: following the conventions of ref. 3, it is defined as a function of the parameters as

$$N_R = x + 2v_2 + 4v_0 + 8y_1 + 16v_1 + 32y_0 + 64y_2 + 128z \tag{1.13}$$

where all the parameters entering this formula take the values 0 or 1.

"Peripheral Automata." The example of Section 1.1 can be viewed as a particular case among the more general 1D PCA described here, namely those where the state of a spin at time t depends only on its neighbors at time $t-1$, and not on itself. The term "peripheral" is generally given to these automata.[2,10] This enforces the following condition on the conditional probability:

$$P(S_3/S_1, S_0, S_2) = P(S_3/S_1, -S_0, S_2) \tag{1.14}$$

which reads

$$x = v_0, \qquad z = y_0, \qquad y_1 = v_2, \qquad y_2 = v_1 \tag{1.15}$$

This results in the cancellation of some of the coupling constants:

$$H_0 = 0, \qquad K_{01} = K_{02} = K_{03} = 0, \qquad K_1 = K_2 = K_3 = 0, \qquad L = 0 \tag{1.16}$$

As a consequence, the 2D lattice of Fig. 2a splits into two *independent* sublattices, as depicted in Fig. 2b. As expected, each one is a triangular sublattice identical to the of Fig. 1a. Thus, the evolution of a peripheral PCA can be viewed as the evolution of two independent two-step PCA of the type

Table II. The 16 "Peripheral" Deterministic Rules[a]

(x, z, y_1, y_2)	N_R	Boolean form	Class	Comment
(0000)	0	0	I	Affine, DB
(1111)	255	1	I	Affine, DB
(0100)	160	$a_1 a_2$	I	DB
(0111)	250	$a_1 + a_2$	I	DB
(1000)	5	$\bar{a}_1 \bar{a}_2$	II	DB
(1011)	95	$\bar{a}_1 + \bar{a}_2$	II	DB
(0011)	90	$a_1 \bar{a}_2 + \bar{a}_1 a_2$	III	
(1100)	165	$\bar{a}_1 \bar{a}_2 + a_1 a_2$	III	
(0010)	10	$\bar{a}_1 a_2$	II	QH
(0001)	80	$a_1 \bar{a}_2$	II	QH
(1110)	175	$\bar{a}_1 + a_2$	II	QH
(1101)	245	$a_1 + \bar{a}_2$	II	QH
(0110)	170	a_2	II	Linear, QH
(0101)	240	a_1	II	Linear, QH
(1010)	15	$\bar{a}_1$	II	Linear, QH
(1001)	85	$\bar{a}_2$	II	Linear, QH

[a] The last column indicates rules which are "affine" or "linear" or satisfy the "quasi-Hamiltonian" (QH) or "detailed balance" (DB) property.

described in Section 1.1. The deterministic limits of such PCA have rule numbers [using (1.13) and (1.15)]

$$N_R = 5x + 10y_1 + 80y_2 + 160z \tag{1.17}$$

These deterministic "peripheral" rules are enumerated in Table II, together with their Boolean decompositions and with their "classes" (in Wolfram's sense[3]), which gives qualitative information on their complexity.[4] We also indicate whether they belong to some of the remarkable classes studied in the following: "quasi-Hamiltonian" rules (Section 1.6) or "affine" ones (Section 2.1). We will devote special attention throughout this paper to the isotropic case $y_1 = y_2$, whose phase diagram is given in Section 1.6 (Fig. 5b).

[4] These four classes characterize the states reached when starting from a random initial one: (I) homogeneous state, (II) separated stable or periodic structures, (III) chaotic pattern, (IV) complex localized structures.

1.4. Other One-Dimensional Examples

1.4.1. Multiple-States PCA. The previous examples can be extended in a straightforward way to the case where each variable $S_{i,t}$ can take q different values ("colors"). The associated spin models are generalized anisotropic q-state Potts model.[20] Explicit formulas for this mapping in particular cases, together with studies of the disorder varieties of the Potts model, can be found in refs. 8 and 21–23.

1.4.2. "Staggered" Rules. This kind of PCA rule can be mapped onto a frequently studied type of anisotropic model: Ising (or Potts) models on the checkerboard lattice. Consider a linear chain of sites which evolve simultaneously at each time step, with the following "alternating" rule: at even time steps, sites $2n$ and $2n+1$ group together and change their states according to conditional probabilities $P(S_{2n,t+1}, S_{2n+1,t+1}/S_{2n,t}, S_{2n+1,t})$. At odd time steps, sites $2n$ and $2n-1$ group together, and evolve according to the same conditional probabilities. The "space-time lattice" generated this way has a "checkerboard" structure (Fig. 3), each elementary plaquette (hatched square) supporting in general all possible types of spin interactions. They are linked by the "disorder condition" for the Boltzmann weight $W(S_1', S_2'/S_1, S_2)$, which stems from the normalization of probability:

$$\sum_{S_1', S_2'} W(S_1', S_2' | S_1, S_2) = \text{independent of } S_1, S_2 \tag{1.18}$$

Once again, this is the criterion used in ref. 14 to find the disorder solutions of the checkerboard Potts model.

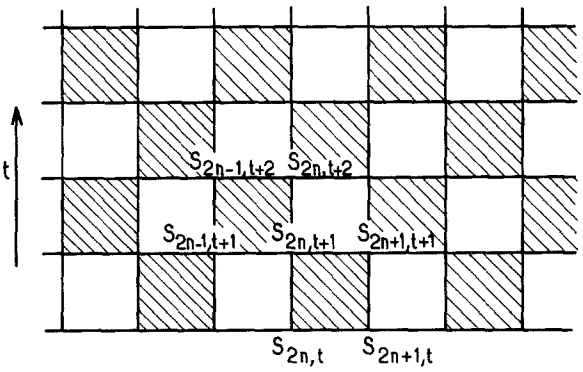

Fig. 3. Checkerboard space-time lattice associated with "staggered' PCA rules.

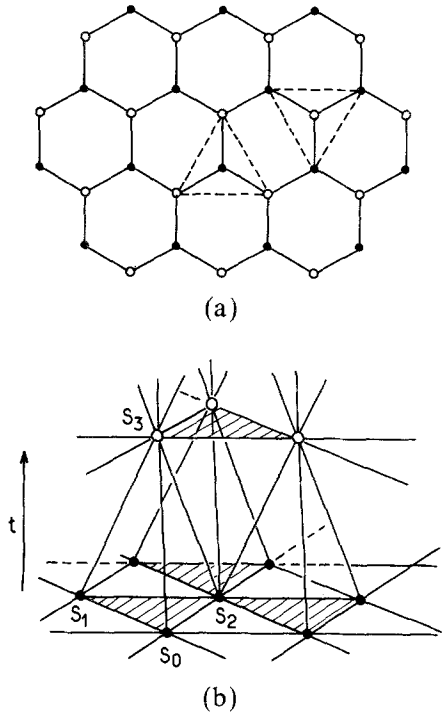

Fig. 4. (a) The honeycomb lattice and its two triangular sublattices. (b) The space-time hcp lattice associated with the two-dimensional PCA described in the text (from ref. 11).

1.5. A 2D PCA and Its Associated 3D Spin Model

We shall finally illustrate the mapping of a 2D PCA onto a 3D equilibrium spin model by a simple example. It was introduced, in a particular case, by Welberry and Miller[5] as a three-dimensional model of crystal growth, and has been recently revisited by Domany[11] in the very special case where the detailed balance principle is satisfied (see below, Section 1.6). This example can be viewed as a natural generalization to higher dimensions of the two-step ("peripheral") PCA of Section 1.1. Consider a 2D honeycomb lattice with binary variables $S_{i,t}$ and divide it into two triangular sublattices,[5] as depicted in Fig. 4a. At even (resp. odd) time steps, the black (resp. white) spins change their states according to probabilistic rules depending on the states of their three white (resp. black)

[5] Note that this is not the original way in which Welberry and Miller introduced this model. They rather viewed the hcp lattice as generated by a 2D crystal-growth model evolving along the (III) direction of a cubic lattice.

nearest neighbors, which remain unchanged. The rule is thus characterized by the eight conditional probabilities $P(S_3/S_1, S_0, S_2)$. The three-dimensional space-time lattice generated by this evolution, depicted on Fig. 4b, is made of alternating 2D layers (the black and white triangular sublattices); the elementary cell is the up-pointing tetrahedron (S_3, S_1, S_0, S_2): one thus recognizes a hexagonal close-packed structure. The associated 3D equilibrium Hamiltonian involves all possible couplings between the spins of an elementary tetrahedron. The coupling constants are the same functions of the eight parameters of the PCA as for the general 1D PCA of Section 1.3 [Eq. (A.11) of Appendix A].

Other examples of 2D PCA can be given leading to 3D equilibrium spin models satisfying a "disorder condition." Some of them can be viewed as 3D generalizations of the checkerboard-type models in two dimensions, and thus correspond to "staggered" PCA rules. We refer to refs. 14, 24, and 25 for further details.

1.6. Symmetries of PCA and the Existence of an Asymptotic Measure

1.6.1. Elementary Symmetries. Let us briefly summarize some general symmetry properties, which relate different evolution rules together.

Spin-Reverse Symmetry ("conjugation"): To any PCA rule, one can associate the rule for which $+1$'s and -1's are simply exchanged. For the PCA of Sections 1.3 and 1.5 this amounts to the following change in the parameters:

$$z \leftrightarrow 1 - x, \qquad v_i \leftrightarrow 1 - y_i \qquad \text{for all } i \tag{1.19}$$

Up to this exchange, the two rules have of course exactly identical properties. They have in particular the same degree of complexity, and belong to the same "class" in Wolfram's sense. The rules which satisfy

$$z + x = 1, \qquad y_i + v_i = 1 \qquad \text{for all } i \tag{1.20}$$

are invariant by conjugation, and so is their associated equilibrium spin model (it involves no couplings between an odd number of spins).

Left/Right Symmetry ("reflection"): One can associate to each 1D PCA rule of Section 1.3 its "image in a mirror" through

$$y_1 \leftrightarrow y_2, \qquad v_1 \leftrightarrow v_2 \tag{1.21}$$

This kind of spatial symmetry can be immediately extended to the 2D case. Rules invariant under reflection will be called "isotropic" in the following.

Ferromagnetic/Antiferromagnetic Symmetry. This applies to conjugation-invariant rules. It is not generally discussed in the context of PCA, but is quite naturally suggested by the mapping onto a spin model. With each space-time "history" $\{S_{i,t}\}$ is associated a transformed one $\{\tilde{S}_{i,t}\}$ defined by

$$\text{for all } i: \quad \tilde{S}_{i,t} = S_{i,t} \quad \text{for } t \text{ even}$$
$$= -S_{i,t} \quad \text{for } t \text{ odd} \tag{1.22}$$

$S_{i,t}$ is thus obtained by alternatively flipping the layers of the space-time lattice. With a given PCA rule, one would like to associate a transformed rule which would give the history $\{S_{i,t}\}$ the same probability as the original rule to $\{S_{i,t}\}$. By looking at this requirement at two successive time steps, it is easily seen that this is only possible for *conjugation-invariant rules.* For these rules, it amounts to the following change:

$$x \to 1-x=z, \qquad z \to 1-z=x, \qquad y_i \to 1-y_i=v_i, \qquad v_i \to 1-v_i=y_i \tag{1.23}$$

which is such that between-layer coupling constants of the equilibrium model change their signs, while inside-layer ones do not [cf. Eq. (A.11)]. Thus, it can be seen as a ferro/antiferro symmetry of this model. Note that this transformation can induce significant qualitative changes in the pattern generated by the two rules, starting from a *fixed* initial configuration, but that their *statistical* properties should be identical. It is, in particular, a useful symmetry to keep in mind when dealing with the critical properties of conjugation-invariant PCA, since it relates one to the other the "ferromagnetic" and "antiferromagnetic" critical values of the parameters. In the deterministic limits (1.13), it relates one of the 16 conjugation-invariant rules N_R to $255-N_R$, or, explicitly, (15, 240), (85, 170), (23, 232), (43, 212), (113, 142), (51, 204), (77, 178), (105, 250). All these rules belong to class II, except the last one, which is chaotic (class III). It can be checked that they have indeed identical statistical properties,[6] and we therefore emphasize that these equivalences should be taken into account when defining "minimal representing rule numbers" (equivalence classes under simple symmetries).[(2)]

1.6.2. Detailed Balance and Time Reversal. Whether an asymptotic measure can be defined over the configurations of the D-dimensional array of spins for a given PCA is an important question, and, in general, a difficult one. There is, however, a well-understood situation,

[6] Simulations of the patterns generated by 1D deterministic rules, together with their statistical properties, can be found in the Appendix of ref. 2.

namely when the rule satisfy the *detailed balance* principle. This requires the existence of a hamiltonian $\mathscr{H}_D$ over the D-dimensional array of spins, such that

$$\prod_i \frac{P(S_i'|\{S_j\})}{P(S_i|\{S_j'\})} = \exp(\beta[\mathscr{H}_D[\{S_i\}] - \mathscr{H}_D[\{S_i'\}]]) \tag{1.24}$$

for any two configurations (S_i) and (S_i'). This condition ensures that the Gibbs measure $\exp[-\beta\mathscr{H}_D]$ is approached asymptotically as time goes to infinity: the PCA thus describes the parallel dynamics of the D-dimensional spin model with Hamiltonian $\mathscr{H}_D$.

The detailed balance condition (1.24) is easily solved[26,12] for the 1D PCA of Section 1.3. Writing the conditional probability $P(S_3/S_1, S_0, S_2)$ under the form of Eq. (A.10), one gets

$$\prod_i P(S_i'/\{S_j\}) = 1/\lambda \cdot \exp\Big[G_0(\{S\}) + \sum_i S_i'(H_3 + K_{13}S_{i-1} + K_{03}S_i + K_{23}S_{i+1} + G_1(\{S\}))\Big] \tag{1.25}$$

where the functions G_0 and G_1 have been introduced to simplify notations (G_1 contains only two- and three-spin products). This leads to

$$\prod_i \frac{P(S_i'|\{S_j\})}{P(S_i|\{S_j'\})} = \exp\Big[G_0(\{S\}) - G_0(\{S'\}) + \sum_i [H_3(S_i' - S_i) + (K_{13} - K_{23})\, S_i'(S_{i-1} - S_{i+1}) + S_i' G_1(\{S\}) - S_i G_1(\{S'\})]\Big] \tag{1.26}$$

It is then clear that (1.24) is satisfied if and only if G_1 vanishes identically, and $K_{13} = K_{23}$. The detailed balance condition for the 1D PCA thus reads[12,26]

$$\begin{aligned} K_{13} &= K_{23} \\ K_0 &= K_1 = K_2 = L = 0 \end{aligned} \tag{1.27}$$

The one-dimensional Hamiltonian defining the Gibbs measure is easily obtained from (1.26), and reads, up to an additive constant,

$$-\beta\mathscr{H}_D = -G_0 + H_3 \sum_i S_i$$

$$= (H_3 - H_0 - H_1 - H_2) \sum_i S_i - (K_{01} + K_{02}) \sum_i S_i S_{i+1}$$

$$- K_{12} \sum_i S_i S_{i+2} - K_3 \sum_i S_{i-1} S_i S_{i+1} \tag{1.28}$$

Conversely, starting from a given Hamiltonian, one can construct along these lines a PCA rule describing its parallel dynamics (see ref. 45 for illustrations). (Note, however, that if one insists on keeping the elementary cell of Fig. 2a, the coupling constants K_0 and K_{12} cannot take arbitrary values.)

In fact, as expected, the detailed balance condition (1.27) is equivalent to *time-reversal invariance*. This is most easily seen on the associated equilibrium spin model. The elementary cell corresponding to the time-reversed evolution is depicted in Fig. 5a: it involves the couplings between the spins $(S_{i,t}, S_{i-1,t+1}, S_{i,t+1}, S_{i+1,t+1})$. Constraining this elementary cell to be identical to the direct one is obviously equivalent to the detailed balance condition (1.27).

It is worthwhile at this step to deal more explicitly with an example[10] which will often be considered in the following, namely the "peripheral" PCA of Section 1.1 in the isotropic case $y_1 = y_2$. For further reference, the three-parameter (z, x, y) phase diagram of these PCA is depicted in Fig. 5b. [Note that this phase diagram has symmetry properties under conjugation and also when $y = 1/2$, $z + x = 2$ (segment CC') under ferro/antiferro symmetry.] Detailed balance is satisfied when the three-spin coupling constant K_0 vanishes, namely [cf. Eq. (A.3)]

$$\frac{z}{1-z}\frac{x}{1-x} = \left(\frac{y}{1-y}\right)^2 \tag{1.29}$$

In order to figure out the location of this manifold in the phase diagram of Fig. 5b, the six edges of the cube as well as the segment CC' which are included into this manifold have been drawn in dashed-dotted. (It will be shown below that CC' corresponds to the remarkable class of "linear" PCA.) When (1.29) is satisfied, the PCA rule describes the parallel dynamics in two steps (alternating updating of odd- and even-indexed spins) of the following one-dimensional Ising model:

$$-\beta\mathscr{H} = \sum_i (JS_iS_{i+1} + BS_i) \tag{1.30}$$

The three parameters x, y, and z are determined from the couplings J and B through (1.29) and

$$\frac{zx(1-z)(1-x)}{[y(1-y)]^2} = e^{8K_{12}} = e^{-8J}$$
$$\left(\frac{1-z}{x}\right)^4 = e^{8(H_1+H_2-H_3)} = e^{-8B} \tag{1.31}$$

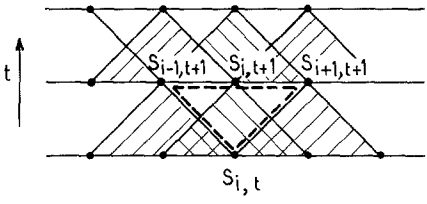

(a)

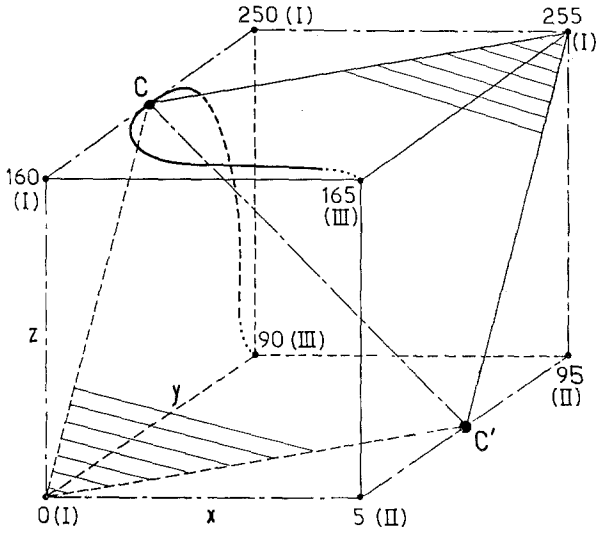

(b)

Fig. 5. (a) The elementary cell (delimited by the dashed lines) corresponds to the time-reversed evolution of the PCA of Section 1.3. (b) Phase diagram of the PCA of Section 1.1 with $y_1 = y_2 (= y)$. The rule number and "class" have been indicated at each (deterministic) corner. The surface (1.29), on which detailed balanced is satisfied, contains all dashed-dotted lines. The hatched plane corresponds to affine rules (and segment CC' to linear ones). The equivalence with directed percolation holds on the faces $x = 0$ and $z = 1$[10]: the corresponding critical curve is depicted as given in ref. 10 (dots indicate numerical indetermination).

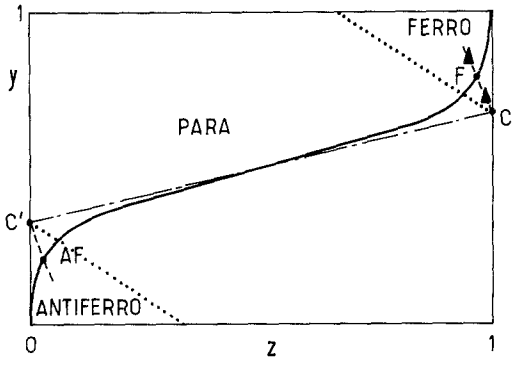

(c)

Fig. 5 (*continued*). (c) Phase diagram of the Welberry and Miller model: detailed balance is satisfied along the solid curve, the rule is linear along the dashed-dotted line. Critical boundaries: dotted lines: mean-field approximation; dashed curves: expected location (critical points C, C' and F, AF are exactly known; triangles were found numerically in ref. 5).

The transition rate between two successive configurations $\{S_i^t\}$ and $\{S_i^{t+1}\}$ thus reads, as expected (at even time steps),

$$w(t \to t+1) = \exp[-\beta \mathscr{H}(\{S_i^{t+1}\})] \prod_{\substack{i \\ \text{odd}}} \frac{\delta(S_i^t, S_i^{t+1})}{N[\{S\}]} \tag{1.32}$$

where N is a normalization factor involving the fixed spins only. Segment CC' (on which spin-reversal invariance holds) corresponds to the dynamics of the Ising model in zero magnetic field. A phase transition is thus expected at zero temperature, that is, for $y = 1/2$ and $(x, z) = (0, 1)$ or $(1, 0)$. Indeed, we will show in Section 2.2 that points C and C' are critical points, and discuss the corresponding critical behavior.

For the 2D PCA of Section 1.5, the detailed balance condition takes a form slightly different from (1.27). Indeed, in this case, the spin S_0 is on the same footing as S_1 and S_2, and a supplementary condition must thus be added to (1.27), which becomes

$$\begin{aligned} K_{03} &= K_{13} = K_{23} \\ K_0 &= K_1 = K_2 = L = 0 \end{aligned} \tag{1.33}$$

In the following we shall study in some detail those of the 2D PCA which are invariant by conjugation and isotropic, i.e., such that $x = 1 - z$, $y_0 = y_1 = y_2 = 1 - v_0 = 1 - v_1 = 1 - v_2$ (denoted by y). This is the "crystal

growth model" originally considered by Welberry and Miller.[5] For this model, the detailed balance condition becomes simply $L=0$, which reads

$$\frac{z}{1-z}=\left(\frac{y}{1-y}\right)^3 \tag{1.34}$$

This is the plain curve appearing in the phase diagram of the model depicted in Fig. 5c (note that this phase diagram has the ferro/antiferro symmetry property). When (1.34) is satisfied, the PCA describes the two-step parallel dynamics of a *honeycomb* Ising model, as studied in detail in refs. 11 and 13. Adapting to this case the analysis made above, the Hamiltonian of this honeycomb model is easily found to be

$$-\beta\mathscr{H}=\sum_{\langle ij\rangle} S_i\sigma_j \tag{1.35}$$

where K denotes $K_{03}=K_{13}=K_{23}$ and S_i, σ_i are the spins of the two triangular sublattices of Fig. 4a. The transition rate between two configurations has a form similar to (1.32); the parameters y and z are related to K through

$$y=\frac{e^K}{2\cosh K}, \qquad z=\frac{e^{3K}}{2\cosh(3K)} \tag{1.36}$$

The underlying equilibrium model on the hcp lattice involves only two-spin coupling constants: between-plane ones $K_{03}=K_{13}=K_{23}=K$, and inside-plane ones $K_{12}=K_{01}=K_{02}$ (denoted by K'). The "disorder condition" links K with K' reads in explicit form

$$\exp(4K')=\cosh(K)/\cosh(3K) \tag{1.37}$$

Note, in passing, that this means that $-K'$ is obtained from the K's through a star–triangle transformation. This is clearly expected from the general form (1.8) of the "disorder condition," which states that the inside-plane coupling constants obtained when summing over S_3 have to compensate the K'.

A dynamical phase transition is expected to occur for the values of (y, z) corresponding to the (ferromagnetic and antiferromagnetic) critical points of the honeycomb Ising model (1.25). These are the points F and AF in the phase diagram of Fig. 5c. Thus, in this case, the critical and "disorder" varieties of the associated hcp Ising model *do have an intersection at nonzero temperature*: we will come back to this point in Section 2.4.

1.6.3. "Quasi-Hamiltonian" PCA. Finally, we want to point out the existence of a slightly more general class of PCA than those satisfying detailed balance, and for which a Hamiltonian over the configurations can nevertheless be defined. Consider again the time-reversed elementary cell of Fig. 5a: instead of exact time-reversal invariance, let us constrain this cell to coincide with the direct one only *up to a left/right symmetry*. This no longer requires K_{13} to be equal to K_{23}, and replaces condition (1.27) by the less constraining one

$$L = K_0 = K_1 = K_2 = 0 \tag{1.38}$$

Stated differently, this means that the time-reversed Boltzmann weight itself (which involves the spins $S_{i,t}$, $S_{i-1,t+1}$, $S_{i,t+1}$, $S_{i+1,t+1}$) satisfies the disorder condition (1.8) when summed over $S_{i,t}$. We will show in Section 2 (Sections 2.2 and 2.4) that, when this condition is satisfied, all equal-time correlation functions of the PCA are equal to the *equilibrium* correlation functions of a D-dimensional spin model with Hamiltonian $\mathscr{H}_D$ given by (1.28). However, *the steady state carries a nonzero current when* $K_{13} \neq K_{23}$ (that is, when the detailed balance principle is not satisfied). Indeed, because of the anisotropy of the rule, its time development displays some privileged velocities: one has to supplement the Gibbs measure $\exp(-\beta\mathscr{H}_D)$ with a "current at infinity" to define the asymptotic properties of the configurations (in a way very similar to the case of a *biased* random walk). A more detailed study of such anisotropy-dependent properties will be made in Section 2.2 for a specific example. Similar situations displaying a current-carrying steady state have been recently investigated in ref. 62.

We choose to call "quasi-Hamiltonian automata" the PCA satisfying this property. Provided the Hamiltonian $\mathscr{H}_D$ does not have too unusual properties, it is clear that such PCA cannot display very complex time developments such as chaotic behaviors: thus, they can only belong to classes I or II in Wolfram's sense. It is interesting in this respect to look for the deterministic rules which are limits of "quasi-Hamiltonian" PCA: this is performed in Appendix C in an exhaustive way. Rather surprisingly, it is found that as much as half of the 256 deterministic rules of Section of Section 1.3 are quasi-Hamiltonian ones, and indeed belong[7] either to class I or to class II. Another half of the remaining ones exhibit a complex (class III) behavior.

[7] A privileged direction, revealing a current at infinity, is clearly seen in the patterns generated by most of these class II rules. Notice that it does not always coincide with the "timelike" direction, even in a deterministic limits (see, e.g., rules $N_R = 3$, 7, 27, 35, etc.).

2. DYNAMICAL BEHAVIOR: CORRELATION FUNCTIONS, PHASE TRANSITIONS

In this part, it is shown how the equivalence between D-dimensional PCA and $(D+1)$-dimensional equilibrium spin models can be used in the calculation of time-dependent correlation functions. Diagrammatic and decimation techniques are used, which have been previously introduced for the purpose of expansions around "disorder solutions" of spin models.[27-30,25] The evolution of the time-dependent magnetization $m(t)$ is considered in Section 2.1: this leads to singling out a particular class of PCA, which we call "affine" ones,[22,12,25] for which $m(t)$ can be exactly calculated. It is shown how a mean-field calculation of $m(t)$ can be performed in other cases, and the resulting mean-field approximations to the phase diagrams of Figs. 5b and 5c are discussed. Section 2.2 is devoted to the detailed study of a specific example for which the two-point correlation functions can be exactly calculated, together with the "effective velocity of sound" characterizing the diffusion of an initial excitation. It is shown in Section 2.3 that this exact calculation is in fact possible in principle for all affine PCA. Correlation functions for "quasi-Hamiltonian" rules are studied in Section 2.4, thus providing a justification of the discussion of Section 1.6. Finally, we make some remarks in Section 2.5 on the general nonlinear case.

Particular attention is payed in all these sections to the phase-transitions of PCA and their universality classes. As we shall see, the mapping onto an equilibrium spin model is a very efficient rool for analytical studies of this point, especially by allowing field-theoretic approaches.

2.1. Single-Point Correlation Functions, Magnetization

Even the evolution of the simplest quantity, namely the single-point correlation function, is coupled through a hierarchy of equations to more complicated correlation functions. Indeed, writing the conditional probability under the form

$$P(S_{i,t+1}/(S_{j,t})) = 1/2[1 + S_{i,t+1}F((S_{j,t}))] \tag{2.1}$$

one gets

$$\sum_{S'=\pm 1} S'P(S'/(S_j)) = F((S_j)) \tag{2.2}$$

which involves in general multispin products: taking the average over space-time histories thus relates $\langle S_{i,t} \rangle$ to higher-order equal-time

correlation functions.[27] For the "peripheral" PCA defined by (1.1), for example, one obtains

$$\langle S_{i,t}\rangle = [V + U\langle S_{i-1,t}S_{i+1,t}\rangle]/[1-(T1+T2)] \tag{2.3}$$

which is valid when $\langle S(t+1)\rangle = \langle S(t)\rangle$, that is, far from the boundary layer.

2.1.1. Affine PCA. However, there exists a simple case in which this hierarchy appears in closed form, namely when $F(S)$ is an affine function of the spins:

$$F((S_j)) = V + \sum_j T_j S_{j,t} \tag{2.4}$$

We choose to call such rules "*affine PCA*" ("*linear PCA*" when, in addition, one has $V=0$). They were first introduced in refs. 12 and 25 (and earlier in ref. 22 in a very particular case). They also reduce in some particular cases to "voters models."[63] Among the general 1D PCA of Section 1.3, the affine ones are defined by [using (A.8)]

$$\begin{aligned} &z + x = y_0 + v_0 = y_1 + v_1 = y_2 + v_2 \\ &x - z = v_0 + v_1 + v_2 - (y_0 + y_1 + y_2) \end{aligned} \tag{2.5}$$

and linearity requires furthermore that $z + x = 1$. (These conditions take the same form for the 2D PCA of Section 1.5.) In the deterministic limits, one finds only eight rules satisfying (2.5): six of them are "peripheral" ones and have been already mentioned in Table II. The remaining two are rules 204 (identity a_0) and 51 (complementation a_0). One thus sees that the eight deterministic affine rules are the elementary Boolean operations and their transforms by conjugation. When restricted to the peripheral PCA of Section 1.1, Condition (2.5) defines a hyperplane:

$$z + x = y_1 + y_2 \tag{2.6}$$

which, in the isotropic case $y_1 = y_2$, is the plane depicted in the phase diagram of Fig. 5b. Note that, for these "peripheral" PCA, linearity implies necessarily the "quasi-Hamiltonian" property, which is not true in more general cases. The 2D PCA whose phase diagram is given in Fig. 5c are linear along the straight line $1 + z = 3y$.

For affine PCA, the time-dependent magnetization, defined by

$$m(t) = \frac{1}{N}\sum_i \sum_{\{S_{j,\tau}\}} S_{i,t} \prod_{\substack{j \\ \tau < t}} P(S_{j,\tau} | \{S_{k,\tau-1}\}) \tag{2.7}$$

can be calculated exactly. Using (2.2), one readily obtains that $m(t)$ follows a simple exponential relaxation law:

$$\frac{m(t)-m_\infty}{m(0)-m_\infty}=e^{-t/t_R}$$

$$t_R^{-1}=-\ln\sum_j T_j \tag{2.8}$$

$$m_\infty=\frac{V}{1-\sum_j T_j}\equiv\langle S_{i,t}\rangle$$

Equation (2.8) is valid when $1>1-\sum_j T_j>0$: in the opposite case, an oscillatory factor appears in front of the exponential. One can check that $1-\sum_j T_j$ remains nonzero as long as V does: the phase transition which occurs when these two parameters simultaneously vanish will be studied in Sections 2.2 and 2.3. Expression (2.8) for the relaxation time of $m(t)$ then displays the usual phenomenon of critical slowing down.

2.1.2. "Mean-Field" Approach to the Nonlinear Cases. A mean-field-type approximation can be used to study the time-dependent magnetization in the nonlinear cases.[1,26,31] It simply consists in forgetting the correlations between the evolution of the different spins, and thus decoupling the above hierarchy (this approximation is, as usual, exact in the limit of infinite coordination[26]). The time dependence of $m(t)$ is then approximated by a nonlinear mapping obtained simply by replacing all the spins $(S_{j,t})$ in (2.1) by $m(t)$, namely

$$\begin{aligned} m(t+1)&=F[(m(t))]\\ &=V+\left(\sum_i T_i\right)m(t)+\left(\sum_i U_i\right)m(t)^2+Wm(t)^3 \end{aligned} \tag{2.9}$$

Notice that this approximation is exact for affine PCA.

For the PCA of Fig. 5b, (2.9) reads

$$m(t+1)=[(z+x-2y)/2]\,m(t)^2+(z-x)\,m(t)+(z+x+2y-2)/2 \tag{2.10}$$

The study of the critical points of this mapping provides us with a mean-field approximation of the phase diagram of Fig. 5b. The discriminant reads

$$D_m(x,y,z)=1+4[y(y-1)+x(1-z)]>0 \tag{2.11}$$

and thus one has in general two fixed points (m_-, m_+). One is thus led to

separate different regions, depending on the value of the derivative F'_∞ at these fixed points:

1. $F'_\infty = +1$ defines the critical boundary on which both m_- and m_+ reach the value -1. This is equivalent to $D_m(x, y, z) = 0$; however, the intersection of this manifold with the physical cube $0 \leqslant x, y, z \leqslant 1$ reduces to the lines $(x = 0, y = 1/2)$ and $(z = 1, y = 1/2)$ (which meet at point C): these are the mean-field approximations of the critical lines depicted (from numerical simulations) in Fig. 5b.

2. $F'_\infty = -1$ amount to $D_m(x, y, z) = 4$, and defines another critical surface which includes point C'. In the domain limited by this surface and containing rules $N_R = 5$ and 95, the mean-field magnetization $m(t)$ enters a 2-cycle (m_-, m_+), while in the other half of the cube an asymptotic magnetization is reached. However, numerical simulations indicate that this critical surface is apparently an artefact of the mean-field approach, and in fact reduces to the single point C' (no transition to a 2-cycle is found).

For the 2D PCA of Fig. 5c, (2.9) reads

$$m(t+1) = 3(z + y - 1)\, m(t)/2 + (z - 3y + 1)\, m(t)^3/2 \qquad (2.12)$$

and one thus gets three mean-field phases delimited by critical lines on which $F'_\infty = +1$, namely:

1. $z + y > 5/3$: "ferromagnetic" phase, for which the asymptotic magnetization is given by $m_\infty^2 = (5 - 3z - 3y)/(z - 3y + 1)$.

2. $1/3 < z + y < 5/3$: "paramagnetic" phase, in which the mean-field asymptotic magnetization vanishes.

3. $z + y < 1/3$: "antiferromagnetic" phase (deduced from the ferromagnetic one by the ferro/antiferro symmetry), with opposite magnetizations $\pm m_\infty$ on successive layers, given by $m_\infty^2 = (1 - 3z - 3y)/(z - 3y + 1)$.

These critical lines are depicted in Fig. 5c: thus, in this case, the mean-field approach gives a correct qualitative understanding of the phase diagram, even if the precise shape of the critical lines is found to be slightly different. (As expected, only the critical points C and C' of the linear case are correctly given by mean-field theory; remember that points F and AF are exactly known.)

2.2. Two-Point Correlations: A Solvable Case

We will now consider two- (and higher-) point correlation functions, and first study an example where they can be exactly calculated. Such a

calculation was first performed in ref. 22, though with rather different and lengthier methods than the graphical ones that will be introduced here and used in the following sections. Let us consider the "peripheral" PCA of Section 1.1 in the linear case $U = V = 0$. (The associated 2D model is then simply the zero-field triangular Ising model; see Appendix A.) These PCA are "quasi-Hamiltonian" and have the detailed balance property if one imposes furthermore $y_1 = y_2$ (this last case corresponds to the segment CC' in the cubic phase diagram of Fig. 5b). Averaging over space-time histories of the PCA amounts to a summation over spins in the corresponding equilibrium model: indeed, one can adapt the "decimation technique" of Section 1.1 to the calculation of correlation functions, as first shown by Dhar and Maillard[28] (see also ref. 27), and developed in refs. 25, 29, and 30. Consider a given two-point correlation function $\langle S_{i,t} S_{j,t+\tau} \rangle$. Starting from the boundary conditions described in Section 1.1 for the upper layer, one can perform the downward summation over spins (the factor λ obtained for each plaquette will be absorbed in the normalization $1/Z$). This can be done until the spin $S_{j,t+\tau}$ is met: at this step, one has to sum $S_{j,t+\tau} W$ instead of the Boltzmann weight W itself, and thus the disorder condition (1.8) is *a priori* of no help. This generates a cone of plaquettes (the "causality cone" of $S_{j,t+\tau}$) over which decimation cannot *a priori* be performed (see Fig. 6a). However, one can take advantage here of the "pseudosymmetry" property, which allows one to perform the summation over down-pointing triangles, starting from the lower layer of the lattice (with suitable boundary conditions). Again, this generates a "forbidden cone" starting on site (i, t) (Fig. 6a): one is thus led to distinguish between two very different situations:

(i) $(j, t+\tau)$ does not belong to the "causality cone" issued from (i, t): the difference $(i-j, \tau)$ is "spacelike."

(ii) $(j, t+\tau)$ belongs to this cone: $(i-j, \tau)$ is "timelike."

Such a distinction simply reflects the causality properties of the dynamical process.

In case (i), the past cone of $S_{j,t+\tau}$ can be entirely decimated by the upward summation: thus, there only remains a path of links joining (i, t) to $(j, t+\tau)$ along which the two summations meet (Fig. 6a). (The choice of this path is not unique and does not affect the final result.) The correlation function thus has a purely one-dimensional nature, and reads (using standard results)

$$\langle S_{i,t} S_{j,t+\tau} \rangle_{\text{spacelike}} = \prod_{\text{path}} (\pm t_i) \tag{2.13}$$

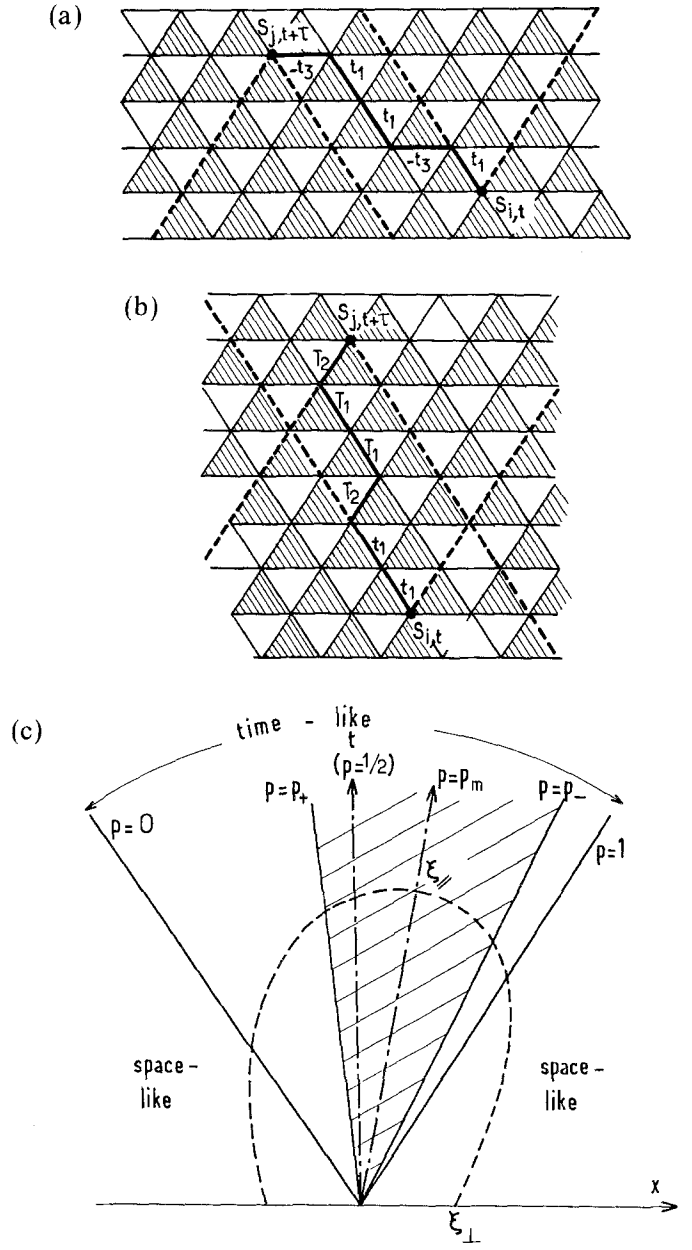

Fig. 6. (a) Spacelike-separated spins: the two cones (dashed lines) do not intersect. The correlation function reduces to a single path weighted by t_i, such as the one depicted. (b) Timelike-separated spins: in this case, the correlation function is a *sum* over directed paths lying inside both cones, weighted as depicted. (c) "Causality cone" (timelike region) and "dynamical cone" (hatched) issued from a given spin $S_{i,t}$. The dashed curve is a schematic contour plot of the correlation length $\xi(p)$.

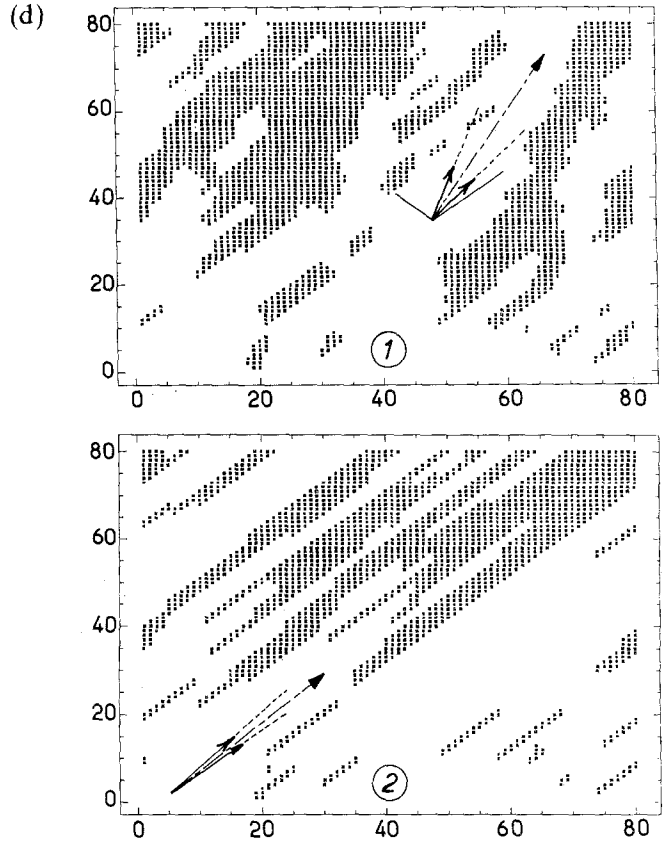

Fig. 6 (*continued*). (d) Pattern generated from the same initial state (two -1's) by linear rules close to criticality ($z=0.99$): (1) $y_1=1-y_2=0.25$, (2) $y_1=1-y_2=0.05$. The velocities V_m (dashed-dotted arrow) and $V_{L,R}$ (solid arrows) are indicated.

[Recall that $t_i=\tanh K_{jk}$; the relation which links the T_i and the t_i is given in Eqs. (A.6)–(A.7) of Appendix A.] In this formula, links K_{13} and K_{23} must be counted with a "plus" sign and links K_{12} with a "minus" sign, since the latter have been involved twice in the decimation process. Using Eq. (A.7) of Appendix A, we obtain in particular for the equal-time correlation length

$$\xi_\perp^{-1}=2\ln\frac{|[1-(T_1-T_2)^2]^{1/2}-[1-(T_1+T_2)^2]^{1/2}|}{2(T_1T_2)^{1/2}} \tag{2.14}$$

(valid for $T_1T_2>0$), which coincides with the result of ref. 22.

Expression (2.13) is the one expected, at least for equal-time

correlation functions, when the detailed balance condition $y_1 = y_2$ is satisfied: it simply means that these correlation functions are the *static* ones of the *one-dimensional* Ising model (1.32) with $B = 0$, whose dynamics is described[8] by the PCA (Section 1.6). It is, however, quite remarkable that, as announced in Section 1.6, such a simple form also holds for the PCA which are only "quasi-Hamiltonian": it will be shown in Section 2.4 that this is indeed a general property.

In case (ii), the problem has been recast into a simpler form by decimation, namely the evaluation of the correlation function for the domain of the space-time lattice obtained by intersection of the two cones (Fig. 6b). As is expected for a timelike correlation function, this domain, while smaller than the whole lattice, has *a priori* the full complexity of a two-dimensional problem. However, it can be solved analytically here, thanks to the *linearity* of the PCA rule. Indeed, when summing over the spin $S_{j,t+\tau}$, one gets, using (2.2)–(2.4),

$$\sum_{S_{j,t+\tau}=\pm 1} S_{j,t+\tau} P(S_{j,t+\tau} \mid S_{j-1,t+\tau-1}, S_{j+1,t+\tau-1}) = T_2 S_{j-1,t+\tau-1} + T_1 S_{j+1,t+\tau-1} \tag{2.15}$$

As a result of the linearity of the rule, only single spins appear in the rhs; thus, the process can be iterated recursively, given rise to a sum over paths joining (i, t) and $(j, t+\tau)$, weighted by the T_i (Fig. 6b). Each of these paths passes at most once on each hatched triangle and cannot take horizontal links. This diagrammatics was originally introduced and studied in refs. 29 and 30 for the purpose of expansions around "disorder solutions" of the 2D Ising model. Here, one has to deal with the boundaries of the domain in a proper way: it is not difficult to realize that, as a result of decimation, the links belonging to the edges of the domain have to be counted with a weight t_i instead of T_i. A bit of combinatorics then leads to our final result for the correlation function:

$$\langle S_{i,t} S_{j,t+\tau} \rangle_{\text{timelike}} = \sum_{n=0}^{n_1} t_1^n T_1^{n_1-n} T_2^{n_2} \binom{n_1+n_2-n-1}{n_2-1} + (1 \leftrightarrow 2) \tag{2.16}$$

where n_1 and n_2 are the numbers of links on the lower edges of the domain ($n_1 = 4$, $n_2 = 2$ in Fig. 6b) and are geometrically related in a simple way to the difference $(i-j, \tau)$. The summation index n counts the fraction of the path which is "adsorbed" on one of the boundaries. Indeed, it is interesting

[8] That K_{12} has to be counted with a minus sign in (2.13) is clearly seen in this case on Eq. (1.28).

to notice that this diagrammatics is very similar to a problem of *directed self-avoiding walks*[32,33] (the different directions being affected with unequal weights) in the presence of a fixed boundary.

2.2.1. Long-Time Behavior. It is most interesting to analyze the long-time behavior of the correlation function (2.16). For this purpose, we set $n_1 = pN$ and $n_2 = (1-p)N$, where $0 < p < 1$, and let N go to infinity: this means that we take $R = i - j$ and T simultaneously large, with a fixed ratio R/T (that is, a fixed "velocity"). (The long-time behavior of a correlation function for a fixed spatial separation is simply recovered for $p = 1/2$). Using the steepest-descent method, we find that the saddle point for the first summation in (2.16) is located at

$$n^*/N = \begin{cases} 0 & \text{if} \quad 0 \leqslant p \leqslant T_1/t_1 = p_+ \\ (pt_1 - T_1)/(t_1 - T_1) & \text{if} \quad 1 \geqslant p \geqslant T_1/t_1 \end{cases} \tag{2.17}$$

An analogous behavior is found for the second summation, replacing (t_1, T_1) by (t_2, T_2), and p by $1-p$. This results in the following dominant behavior of the correlation function for large N:

$$\begin{aligned} 0 \leqslant p \leqslant p_- = T_1 t_1 &: \quad \langle S_{i,t} S_{j,t+\tau} \rangle = (t_2^{1-p}/t_1^p)^N \\ p_- \leqslant p \leqslant p_+ = T_1/t_1 &: \quad \langle S_{i,t} S_{j,t+\tau} \rangle = 2[(T_1/p)^p (T_2/1-p)^{1-p}]^N \\ p_+ \leqslant p \leqslant 1 &: \quad \langle S_{i,t} S_{j,t+\tau} \rangle = (t_1^p/t_2^{1-p})^N \end{aligned} \tag{2.18}$$

Thus, there appears another cone in the space-time lattice (Fig. 6c) outside which the behavior of the correlation function is a simple continuation of the one-dimensional behavior valid in case (i). However, inside this cone the behavior is entirely different, and reflects the dynamical nature of the PCA (or, analogously, the 2D nature of the equilibrium model). Note that, while the "causality cone"—corresponding to a unit velocity (the "speed of light")—has a purely *kinematical* nature, the new cone appearing here is truly *dynamical*. The slopes of its boundaries (easily obtained from p_- and p_+) define two velocities $V_{L,R}$ which play the role of the "speeds of sound" for the left and right propagation of an initial excitation in the PCA. In the context of deterministic CA, these quantities are generally called "left and right Lyapunov exponents."[2] Here, they must be understood in a statistical sense, since an average over space-time histories has been performed. Note that when $y_1 \neq y_2$, the PCA rule is not symmetric under reflection, which results in $p_+ \neq 1 - p_-$, and thus in $V_L \neq V_R$, as expected. The axis of the "dynamical cone" thus makes a finite angle with the time axis (Fig. 6c): this illustrates the fact that a "current at infinity" exists for such PCA.

An interesting feature displayed by Eq. (2.18) is the continuous dependence of the correlation length on the direction of observation (or "velocity") R/τ. Defining ξ for simplicity through $\langle S_{i,t} S_{j,t+\tau} \rangle \sim \exp(N/\xi)$, one gets

$$\xi^{-1}(p) = \begin{cases} |p \ln t_1 - (1-p) \ln t_2| & \text{for } p \leqslant p_- \text{ or } p \geqslant p_+ \\ p \ln T_1 + (1-p) \ln T_2 - p \ln p - (1-p) \ln(1-p) & \text{for } p_- \leqslant p \leqslant p_+ \end{cases} \tag{2.19}$$

A schematic contour plot of this function is displayed in Fig. 6c: the two regimes join up in a smooth way at the boundaries $p = p_+$, p_- of the "dynamical cone"; $\xi(p)$ exhibits a maximum for the direction $p = p_m$ inside this cone given by

$$(1-p_m)/p_m = (1-p_+)/p_- = T_2/T_1, \qquad \xi^{-1}(p_m) = \ln|T_1 + T_2| \tag{2.20}$$

Note that this maximum value is equal to the relaxation time of the magnetization t_R calculated in Section 2.1.

All these features are clearly seen on Fig. 6d, which displays the pattern generated by rules close to criticality ($z = 0.99$) for two different values of the "anisotropy" y_2/y_1, starting from the same initial state. The direction V_m given by (2.20) is indicated and indeed coincides with the mean direction of the propagation (and thus appears as the mean velocity of the "current at infinity"). V_L and V_R give a satisfactory estimation of the width of transverse spreading.

The change of behavior of the correlation function inside the dynamical cone can be seen as a "desorption transition" for the directed SAW problem to which the diagrammatics is related. Indeed, inside this cone the saddle point (2.17) is located at $n^* = 0$ (dominant diagrams thus go directly from one point to the other), while it is located at a finite value of n^* outside the cone (part of the diagram is then "adsorbed" on the boundary).

2.2.2. Phase Transitions. The previous expressions for ξ exhibit a divergence when

$$T_1 + T_2 = 2z - 1 \to +1 \text{ or } -1 \tag{2.21}$$

independently of the value of $y_1 - y_2$ (note that these two critical values are related by the ferro/antiferro symmetry of Section 1.6). Indeed, in these limits, one sees from Eq. (A.7) of Appendix A that t_1, t_2 goes to 1 and

$p_+ \sim p_- \to p_m$. More precisely, setting $\varepsilon = 1 - z$ (we deal with the case where $T_1 + T_2 \to +1$, to fix ideas), one obtains

$$t_1 \sim 1 - 2C\sqrt{\varepsilon}, \qquad t_2 \sim 1 - \frac{2}{C}\sqrt{\varepsilon} \tag{2.22}$$

with $C = [(1 + y_2 - y_1)/(1 + y_1 - y_2)]^{1/2}$. Thus, in the critical limit, the "dynamical cone" reduces to the single direction $p = p_m$ of the space-time lattice. In this direction, the following divergence of the correlation length is found:

$$\xi^{-1}(p) \sim 2\varepsilon \qquad \text{for} \quad 1 - \sqrt{\varepsilon} \leqslant p/p_m \leqslant 1 + \sqrt{\varepsilon} \tag{2.23}$$

i.e., $\xi(p) \sim |z - z_c|^{-\nu_\parallel}$, with $\nu_\parallel = 1$, while, apart from this direction, one obtains

$$\xi^{-1}(p) \sim 2\varepsilon^{1/2}\left(pC + \frac{1-p}{C}\right) \tag{2.24}$$

$\xi(p) \sim |z - z_c|^{-\nu_\perp}$, with $\nu_\perp = 1/2$.

This phase transition deserves several remarks.

1. It has the usual features of a dynamical phase transition: "static" and "dynamic" correlations are characterized by different exponents $\nu_\perp = 1/2$ and $\nu_\parallel = 1$, which assume here their mean-field values[34] and lead to a dynamical exponent $z_d = \nu_\parallel/\nu_\perp = 2$. As will be shown below, *this is a general feature of the phase transitions of linear PCA*[12] (as well as directed SAWs[33]). Note that the exponent $\nu_\parallel$ is observed only in a neighborhood (of size $\sqrt{\varepsilon}$) around the particular "velocity" V_m, which does not coincide in general with the time direction, except when the isotropy condition $y_1 = y_2$ is met.

2. In this last case, the critical rules found here correspond to the points C and C' in the cubic phase diagram of Fig. 5b. As discussed in Section 1.6, the rules on the edges $x = 0$, $z = 1$ and $x = 1$, $z = 0$ satisfy the detailed balance condition and thus describe the dynamics of a one-dimensional Ising model. The phase transitions at C and C' simply reflect the zero-temperature transition of this model. Moreover, it has been shown in ref. 10 that PCA rules lying on the side $x = 0$ of the cube (and their transforms by symmetries) are equivalent to a two-dimensional directed percolation problem, and that point C is the endpoint of a critical line (depicted in Fig. 5b from the numerical determination of ref. 10), which separates, in the sides $x = 0$ or $z = 1$ of the cube, a percolating and a nonpercolating phase. In the nonpercolating ("dry") phase, an initially disordered state evolves to a uniform state containing only -1's, while in the percolating ("wet") phase, a finite magnetization is reached (see the patterns displayed in ref. 59). For the "critical rules" themselves, the magnetization (2.8) has

different limits when the transition $V = 1 - \sum_j T_j = 0$ is approached along different directions in the phase diagram. The fact that the points C, C' do *not* fall in the usual universality class of directed percolation,[35,36] which holds along the rest of this line, is due to the linearity of the rules. Nevertheless, many qualitative features found here, such as direction-dependent properties, are also found in usual directed percolation.[31] Indeed, the edge $x = 0$, $z = 1$ of the cube essentially corresponds to the "exactly solvable model of directed-percolation" of Domany and Kinzel,[37] for which $\nu_\perp = 1$, $\nu_{||} = 2$.

3. Some of the linear rules which do not satisfy detailed balance are critical even in the deterministic limits. This is the case of the peripheral rules (15, 85) and (170, 240) and also, as we shall see in the next section, of the rules 51 and 204, which are linear but not peripheral. Note that these rules are of class II and conserve the magnetization.

4. From the point of view of equilibrium spin models, these critical properties appear at first sight as very intriguing. Indeed, the equilibrium model considered here is nothing but the zero-field triangular Ising model on its "disorder variety." Thus, questions immediately arise: Where does anisotropic scaling come from? Where is the usual logarithmic singularity of the 2D Ising model hidden? These apparent paradoxes have been studied in detail and solved in refs. 29 and 30. The main point is that the critical and disorder varieties of the model have an intersection only at zero temperature (i.e., are *asymptotic* one to the other for infinite values of the coupling constants) which corresponds to the transition described above for the PCA. It can be seen that in this region, the usual logarithmic divergence is replaced by an unusual $\alpha = 1/2$ singularity: this is the result expected on the basis of hyperscaling, since

$$\alpha = 2 - D\nu_\perp - \nu_{||} = 2 - \tfrac{1}{2} - 1 = \tfrac{1}{2} \tag{2.25}$$

This phenomenon was already known in specific applications of the Ising model, such as the roughening transition[38] or some dimer models.[39] Indeed, the genuine critical behavior of an equilibrium model is always deeply modified in the vicinity of its "disorder varieties": we shall come back below to this question, which certainly deserves more careful and systematic study.

2.3. Dynamical Behavior of Linear and Affine PCA

2.3.1. Correlation Functions of Linear PCA. The decimation technique allowing us to calculate correlation functions for the previous

example made use of both the linearity and "quasi-Hamiltonian" nature of the PCA rule. However, as will be shown in this section, the linearity property by itself is sufficient to allow exact calculations of spacelike *and* timelike correlation functions.

Indeed, in the previous section, the "quasi-Hamiltonian" property was used only to perform a supplementary upward decimation, leading to simplified calculations. Suppose one no longer has this extra possibility: continuing the downward decimation gives rise, for linear rules, to a sum over simple graphs, such as the one depicted in Fig. 7a for a two-point function of a general 1D linear PCA. As explained for the case (ii) of Section 2.2, this is due to Eqs. (2.2) and (2.4) (with $V=0$): each graph can pass at most once on each plaquette, and cannot take horizontal links. Each link is

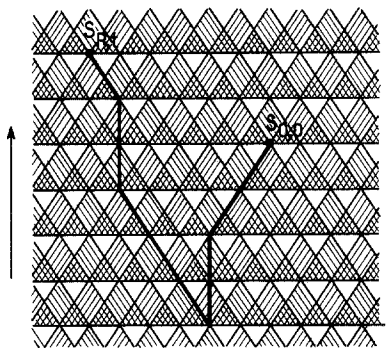

(a)

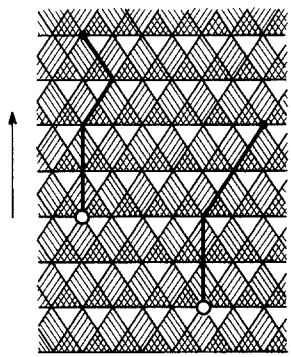

(b)

Fig. 7. (a) In the general linear case (here for $D=1$), the correlation function is a sum over graphs weighted by T_i and obeying the rules given in the text. (b) Graphs ending on a V term (circle) i n the affine case.

affected with the weight T_i corresponding to its direction (i.e., T_1, T_2, or T_0 in the example of Fig. 7a). One thus obtains a summation over $(D+1)$-dimensional admissible graphs (which are in fact a special case of directed SAWs):

$$\langle S_{0,0} S_{R,t} \rangle_{\text{linear PCA}} = \sum_{\Gamma} \prod_{i \in \Gamma} T_i \tag{2.26}$$

When the "pseudosymmetry" condition is satisfied, a partial resummation can be performed among these graphs in order to recover the diagrammatics of Section 2.2.[9]

More explicit expressions can be given for the correlation functions, by noting that (2.26) has a simple interpretation as a *D-dimensional random-walk problem.* Indeed, taking the linear PCA of Section 1.3 as an example, let us consider the one-dimensional random walk in which the walker can jump to the left with weight T_1, to the right with weight T_2, or stay at the same site with weight T_0 (note that, as a slight complication, negative weights can occur). Then, (2.26) is nothing else (up to a normalization factor—see below) than the probability of meeting of two walkers with initial conditions separated by a distance R and a time delay t. Note that, when $|\sum_j T_j| \neq 1$, the random walk has a finite probability of death, so that (2.26) will in general display exponential decrease in space and time, as expected. (As will be shown below, a phase transition arises when $\sum_j T_j \to +1$ or -1.) This random walk problem can generally be solved explicitly in any dimension, for simple enough lattices.[40] The previous section is one of the simplest example of such an explicit solution; others could be given, for example, for the 2D PCA of Section 1.5: one would encounter the same qualitative features, namely the existence of a "dynamical cone" defining left and right "speeds of sound." We want rather to concentrate on the *critical properties* of these linear rules, and will now present simple arguments suggesting that they do not depend on dimensionality.

2.3.2. Phase Transitions and Universality Class of Linear PCA. Let us consider the *relative* walk performed by the vector **AB** joining the two walkers. It is characterized by the following weights:

$$\mathbf{AB} \to \begin{cases} \mathbf{AB}+2 & T_1 T_2 \\ \mathbf{AB}+1 & T_1 T_0 + T_2 T_0 \\ \mathbf{AB} & T_1^2 + T_2^2 + T_0^2 \\ \mathbf{AB}-1 & T_1 T_0 + T_2 T_0 \\ \mathbf{AB}-2 & T_1 T_2 \end{cases} \tag{2.27}$$

[9] This can be checked explicitly and is indeed a remarkable property of the "disorder condition."

The normalization of these weight is $(T_0 + T_1 + T_2)^2$ and the associated randomwalk problem thus involves a probability of death:

$$\Delta = \left[\ln \left(\sum_j T_j \right)^2 \right]^{-1} \tag{2.28}$$

One thus expects linear PCA to have a phase transition when

$$\sum_j T_j \to \pm 1 \tag{2.29}$$

These two critical values are related by the ferro/antiferro symmetry of Section 1.6. They correspond to points C and C' for the 2D PCA whose phase diagram is given in Fig. 5c. Note that, for linear automata of Sections 1.3 and 1.5, $\sum T_j = 2z - 1$: thus, transitions always arise for semideterministic limits in which the PCA has one "absorbing" (or "repelling") state [namely $P(1/111) = 1$ or $P(-1/111) = 1$]. This always corresponds to a zero-temperature transition for the associated model in dimension $D + 1$.

Let us give a simple argument showing that this transition indeed exists, allowing one to calculate the associated critical exponents. The equal-time correlation function $\langle S_0(t)\, S_R(t) \rangle$ is proportional to the total probability of meeting of two walkers initially separated by a distance R. Denoting by $P_1(x, t/R, 0)$ the probability for the relative walk to reach site x for the first time at time t, one thus obtains

$$\langle S_0(t)\, S_R(t) \rangle \propto \int dt'\, P_1(0, t'/R, 0) \tag{2.30}$$

Approximating $P_1(0, t/R, 0)$ by

$$P_1(0, t/R, 0) \sim 1/t^{1 + D/2} \exp(-R^2/Ct - \Delta t) \tag{2.31}$$

and using the saddle-point method in (2.30), one obtains

$$\langle S_0(t)\, S_R(t) \rangle \sim 1/R^{(D-1)/2} \exp[-(\Delta/C)^{1/2} R] \tag{2.32}$$

Thus, the spacelike correlation length diverges in the limit (2.29), with an exponent $\nu_\perp = 1/2$. The algebraic decay at criticality is characterized by $\eta_\perp = (3 - D)/2$. Correlation functions for timelike separations are even simpler to estimate: at criticality, graphs going directly from point $(0, 0)$ to point (R, t) are expected to dominate the large-time behavior for directions R/t inside the "dynamical cone" centered around a velocity V_m. The $\langle S_0(0) \cdot S_R(t) \rangle$ is proportional to the probability for the relative walk to come back at its initial position in a time t; therefore

$$\langle S_0(0)\, S_R(t) \rangle \sim \exp(-\Delta t) \qquad \text{for} \quad R/t \sim V_m \tag{2.33}$$

leading to $\xi_{\|} \sim \Delta^{-\nu_{\|}}$ with $\nu_{\|} = 1$. As explained in the previous section, this timelike behavior is observed only around the particular direction V_m of the space-time lattice; the opening angle of this "dynamical cone" goes to zero at criticality like

$$\xi_{\perp}/\xi_{\|} \sim \Delta^{\nu_{\|} - \nu_{\perp}} = \sqrt{\Delta} \tag{2.34}$$

Thus, the phase transitions of linear PCA are characterized by the mean-field exponents $\nu_{\perp} = 1/2$ and $\nu_{\|} = 1$ in *all* dimensionality.[12] This was to be expected, on the basis of the analogy with directed SAWs. Indeed, this problem is described by an *anisotropic* ϕ^4 $O(N)$ field theory in the limit $N \to 0$, which has been shown[33] to yield the same unmodified mean-field exponents in any dimension. It is in fact quite intriguing to notice[60] that several other (nonlinear) examples of nonequilibrium phase transitions display mean-field critical exponents.[60,61] The above analysis of the linear case could help in the understanding of this point, for which the directed nature of the associated equilibrium model certainly plays a central part.

The universality of the critical properties of linear PCA together with the simplicity of their evolution raises interesting issues concerning the nature of their associated $(D+1)$-dimensional equilibrium models. The transition described here corresponds to a zero-temperature intersection of the critical and disorder varieties of this model. In this limit, anisotropic scaling is found, with a specific heat exponent given by

$$\alpha = 2 - D\nu_{\perp} - \nu_{\|} = 1 - D/2 \tag{2.35}$$

on the basis of hyperscaling, generalizing the $\alpha = 1/2$ "exotic" singularity (2.25) found for the 2D Ising model. This is also confirmed by Cardy's analysis.[33] It is interesting to notice that this singularity has indeed been found for some three-dimensional dimer models.[41] (We emphasize that these results hold despite the analytic character of the free-energy restricted to the disorder variety λ.)

2.3.3. A Remarkable Class of Spin Models. These properties raise the question of what happens when enlarging the equilibrium model outside its disorder variety in such a way that the Boltzmann weight (in its nonexponential form) contains only two-spin products. The intriguing nature of such spin models has been pointed out by Rujan.[12] For $D = 1$, the answer is simple: indeed, adding a term $T_3 S_1 S_2$ to the rhs of Eq. (1.2) allows us to recover the fully anisotropic Ising model, whose formulation as a free-fermion theory in the variables T_i has been explicitly built form the diagrammatics described here in ref. 30. The critical variety of this

enlarged model simply reads $T_1 + T_2 + T_3 = 1$, and its *genuine* logarithmic singularity is quite different from the $\alpha = 1/2$ singularity found in the vicinity of the disorder variety. It appears that the "linear" spin models described here are in some sense a natural extension to higher dimension of the 2D free fermion models, which certainly deserves further study.

2.3.4. Correlation Functions of Affine PCA. The calculation of correlation functions for affine PCA is also possible, though a little more involved, because of the V term in Eq. (2.4). Indeed, when performing the downward decimation, this term gives rise to supplementary graphs (Fig. 7b) in which the "strings" of T_i issued from the two spins simply end on some site, giving rise to a factor V. (Continuing the analogy with directed SAWs, notice that this is quite similar to the des Cloiseaux[42] representation of polymer chains in a solvent, V playing the role of a magnetic field.) Let us sketch how these graphs can be resummed on the example of the equal-time two-point function $\langle S_0(t)\, S_R(t) \rangle$ of a "peripheral" affine PCA (2.6). Denoting by s the number of steps of the shortest "string," one can first resum the contribution of the "free" part of the longest one [beyond the $(s+1)$th step], and obtain for the total contribution of these graphs

$$\frac{V^2}{1-(T_1+T_2)} \sum_s G(s) \tag{2.36}$$

In this expression, $G(s)$ denotes the contribution of all pairs of strings of length s which have not met before s steps. It is given by

$$G(s) = (T_1+T_2)^{2s} \left[1 - \sum_{n=0}^{s} P_1(n/R) \right] \tag{2.37}$$

where $P_1(n/R)$ is the probability of first passage at the origin at "time" n of the relative walk [with normalized weights $T_1 T_2/(T_1+T_2)^2$ and $(T_1^2+T_2^2)/(T_1+T_2)^2$]. Its expression can be found, for example, in ref. 43, thus allowing a complete calculation of the correlation function. However, it is not difficult to see that it does not exhibit any new phase transitions except those of the linear rule $V = 0$. This is presumably a general feature of all affine PCA.

2.4. Dynamical Behavior of "Quasi-Hamiltonian" PCA

In the "quasi-Hamiltonian" case, simultaneous upward and downward decimations can be performed in order to calculate correlation functions,[25,28] as illustrated by the example of Section 2.2.

This shows that n-point *equal-time* correlation functions are n-point functions of a *D-dimensional* equilibrium model. The coupling constants of this equilibrium model are the intraplane coupling constants of the $(D+1)$-dimensional model, but with a signreversal for those which have been involved twice in the decimation process [for this reason, t_3 bonds were affected with a minus sign in formula (2.13)]. This result is the expected one when the PCA rule satisfies, in addition, the detailed balance principle (Section 1.6): then, it describes the parallel dynamics of a D-dimensional model, and equal-time correlation functions are of course the equilibrium correlation functions of this model. Let us illustrate this point on the 2D PCA of Fig. 5c, when it satisfies the detailed balance condition (1.33)–(1.34). Upward and downward decimations on the 3D hcp lattice leave us with a triangular model with coupling constants $-K_{01} = -K_{02} = -K_{12}$ $(= -K')$. As shown in Section 1.6, these coupling constants are precisely those obtained from (K_{03}, K_{13}, K_{23}) through a star–triangle relation. The triangular model obtained is thus equivalent to the honeycomb model (1.35) with coupling constants $K_{03} = K_{13} = K_{23}$ $(= K)$. This is the expected result, since the 2D PCA describes the parallel dynamics of such a model, as explained in Section 1.6.

However, there is no such obvious interpretation of this "dimensional reduction" from $D+1$ to D dimensions when the PCA is *only* "quasi-Hamiltonian" and *does not* satisfy detailed balance. (For the previous 2D PCA, one then obtains an *anisotropic* triangular model with coupling constants $-K_{ij}$.) As already discussed in Section 1.6, this comes from the possibility of defining an asymptotic measure for these rules, provided one supplements it with a "current at infinity."

Simultaneous upward and downward decimations for *unequal time* two-point correlation functions lead to a distinction between the two different situations described in Section 2.2: (i) "spacelike" correlation functions, corresponding to nonintersecting "causality cones"; and (ii) "timelike" correlations (intersecting cones).

The first case is illustrated by Fig. 8a on the example of the 2D PCA of Section 1.5: one is left with a triangular lattice locally distorted by *the surface* of a "pyramid" corresponding to the causality cone issued from the upper point. This pyramid is empty, as a result of upward decimation. Case (ii) is illustated by Fig. 8b: one obtains the two-point function of a lattice made of an infinite triangular layer on which up-pointing and down-pointing pyramids have been glued. All the elementary tetrahedra remain inside the pyramid, and the problem has thus a truly $(D+1)$-dimensional nature, as is expected for a timelike correlation function. However, the resulting lattice has a much smaller size than the full space-time lattice, and this could possibly be used in order to build faster algorithms to compute

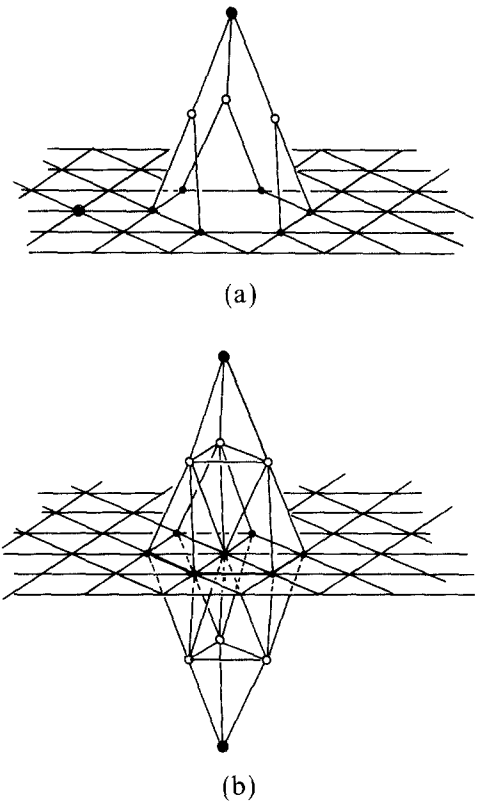

Fig. 8. (a) Spacelike correlation function of a (2D) "quasi-Hamiltonian" PCA. (b) Timelike correlation function of a (2D) "quasi-Hamiltonian" PCA.

these correlations. The method can be generalized to n-point correlation functions: we refer to ref. 25 for a more detailed illustration on 3D examples.

Phase Transitions and Universality Classes. Phase transitions for "quasi-Hamiltonian" PCA can be identified from the critical points of the D-dimensional model found in the calculation of equal-time correlation functions. When $D=1$, we expect this model to have phase transitions only in the limit of zero temperature and thus phase transitions to occur only for *semideterministic limits* of the PCA, as noticed in ref. 26. In other words, the disorder and critical varieties of the $(D+1)$-dimensional equilibrium models are only asymptotic one to the other for infinite values of the coupling constants. These are the features encountered, for

example, in Section 2.2. However, as soon as $D>1$, the underlying D-dimensional model can have a transition at finite temperature, which means that the disorder and critical varieties have *a nontrivial intersection* for finite values of the coupling constants. This is indeed what happens for the 2D PCA of Section 2.5: it is *a priori* obvious when detailed balance is satisfied[5,11] since the honeycomb Ising model undergoes a transition for

$$\begin{aligned} K_F &= 1/2 \cdot \ln(2+\sqrt{3}) \qquad \text{(ferro)} \\ K_{AF} &= -K_F \qquad\qquad\quad \text{(antiferro)} \end{aligned} \tag{2.38}$$

These are the critical points F and AF indicated in the phase diagram of Fig. 5c along the line where detailed balance is satisfied. This suggests that a critical line should exist joining these points to the critical points C and C' found above in the linear limit as indicated by the mean-field theory of Section 2.1. Indeed, two other transition points (depicted by triangles on Fig. 5c) have been determined numerically for $L=0$,[5] which confirms this hypothesis. We deduce from the above analysis that the singularities of equal-time correlation functions at the points F and AF are those of the 2D Ising model:

$$\nu_\perp = 1, \qquad \eta_\perp = 1/4 \tag{2.39}$$

(and, more generally, $\nu_\perp = \nu_D^{\text{eq}}$, $\eta_\perp = \eta_D^{\text{eq}}$). However, timelike correlation functions are expected a different critical behavior, with exponents $\nu_{||}$ and $\eta_{||}$. From the point of view of the $(D+1)$-dimensional equilibrium model, this appears at first sight as utterly paradoxical: it means that the critical behavior at the intersection with the critical variety displays (i) anisotropic scaling of D dimensions versus one, contrarly to the general wisdom about the "irrelevance of anisotropy," and (ii) a free energy *free of any singularity* at the transition (λ is just an algebraic expression).

These questions have been adressed by Domany in his study of the hcp Ising model[11] and answers have been given by Domany,[11] Domany and Gubernatics,[13] Aharony *et al.*,[44] Zimmerman *et al.*,[46] and Auerbach[47] on the basis of Monte Carlo simulations, field-theoretic arguments, and series expansions. It appears that the intersection between the disorder and critical varieties is a *Lifchitz tricritical point.*

This feature is not already apparent at the level of mean-field theory (see Domany[11] and Auerbach[47]), where this point rather appears as a usual Lifchitz point (see Hornreich *et al.*[47]) with continuous transitions. However, as pointed out in ref. 13, this cannot be the whole story, since the upper critical dimension is expected to be $D_c=4$ (instead of $D_c=5$ for a usual Lifchitz point, and the classical values of the exponents for $D=D_c$ should be $\nu_\perp = 1/2$ and $\nu_{||}=1$, as is expected for kinetic Ising models.[34]

We refer to the above papers for details concerning the solution of these puzzles, and will only reproduce here the field-theoretic arguments of ref. 13. The starting point is the following Langevin equation for the field $\phi(\mathbf{x}, t)$:

$$\frac{\partial \phi}{\partial t} = -\frac{\delta H_D}{\delta \varphi} + \eta(x, t) \tag{2.40}$$

where H_D is the Landau–Ginzburg Hamiltonian relevant to the description of the D-dimensional equilibrium model close to criticality:

$$H_D = \tfrac{1}{2}(\nabla_\perp \phi)^2 + \tfrac{1}{2} m \phi^2 + g\phi^4 \tag{2.41}$$

Domany and Gubernatis then make use of the standard method making it possible to express time-dependent correlation functions as static correlations of the $(D+1)$-dimensional effective Hamiltonian[10]:

$$\begin{aligned} H_{D+1} &= \left(\frac{\partial \phi}{\partial t}\right)^2 + \left(\frac{\delta H_D}{\delta \phi}\right)^2 - \frac{\delta^2 H_D}{\delta \phi^2} \\ &= \frac{\mu}{2}(\nabla_\perp \phi)^2 + \frac{1}{2}(\nabla_{||} \phi)^2 + \frac{M}{2}\phi^2 \\ &\quad + \frac{1}{2}(\nabla_\perp^2 \phi)^2 + V\phi^3 \nabla_\perp^2 \phi + G\phi^4 + W\phi^6 + \cdots \end{aligned} \tag{2.42}$$

with $M \sim m^2$, $\mu \sim m$, $G \sim m$. This Hamiltonian is thus expected to describe the critical behavior of the associated $(D+1)$-dimensional model *on its disorder variety*. Indeed, note that the coefficients in Eq. (2.42) are not all independant, being functions of m and g only. This has deep consequences:

1. First, (2.2) has a remarkable symmetry property, namely Parisi–Sourlas supersymmetry[48]; this accounts for the regularity of the freeenergy.

2. Second, at the critical point $m = 0$ of H_D, one observes that the parameters μ and G in (2.42) simultaneously vanish; this identifies the critical point of H_{D+1} as a Lifchitz tricritical point with D "soft" directions. Anisotropic scaling is expected at this point, and the fact that the new terms ϕ^6 and $\phi^3 \nabla_\perp^2 \phi$ become relevant in H_{D+1} accounts for the upper critical dimension $D_c = 4$ and allows one to recover the expected classical values and $4 - \varepsilon$ expansion of the exponents.[44] This approach thus sheds some light on the above puzzles, and demonstrates that the $(D+1)$-dimensional model *is in a complete different universality class when considered on*

[10] See, for example, ref. 64, where this mapping for a continuous field has been extensively studied.

its disorder variety. This raises interesting questions concerning the universal character of this analysis:

3. It suggests that the phase transitions of all $D > 1$ fully probabilistic PCA satisfying detailed balance are described by a Lifchitz point in the associated $(D+1)$-dimensional model.

4. The same conclusion is most likely valid for those PCA which are only "quasi-Hamiltonian": as long as the inside-plane coupling constants remain finite, anisotropy in the D "spatial" directions is expected to be irrelevant: one would thus have a "Lifchitz tricritical surface" in the phase diagram.

5. Finally, one is tempted to ask whether PCA which do not satisfy "pseudosymmetry" could also fall in this universality class, and thus have the critical exponents of kinetic Ising models. We will come back to this point in the next section.

2.5. Some Remarks on the Critical Behavior of Nonlinear PCA

The time evolution of the PCA which are neither "affine" nor "quasi-Hamiltonian" ones has the full complexity—and interest—of nonlinear problems. In these cases, the diagrammatics associated with a given correlation function involves "reproduction" and "recombination" processes in addition to the diffusion and death processes already present for affine rules. These new processes are due to the multispin products (U and W terms) involved in the function $F(S_j)$ of Eq. (2.2) and are illustrated on Fig. 9 for the "peripheral" rules (1.2). The complexity of the evolution results from the combination of these nonlinear elementary processes. One of the simplest illustrations of how they can generate chaotic behavior is provided by the deterministic rule $N_R = 90$ ($x = z = 0$, $y = 1$). In this case, the pattern generated from a single-site seed is simply the self-similar Pascal triangle and the nonlinear superposition of these individual patterns results in the chaotic (class III) behavior observed for a random initial state. In more complicated cases (such as rule $N_R = 30$) an irregular pattern is obtained even from a single-site seed; these processes can also generate soliltonlike interacting structures ($N_R = 110$).

A lot of work has been devoted to the understanding of these nonlinear effects,[2] and many questions remain open. In the following we only want to address some aspects of the problem of phase transitions. Do there exist other universality classes than those of the "linear" rules (behaving as directed SAWs) and "quasi-Hamiltonian" ones (behaving as kinectic Ising models) encountered in the two previous sections?

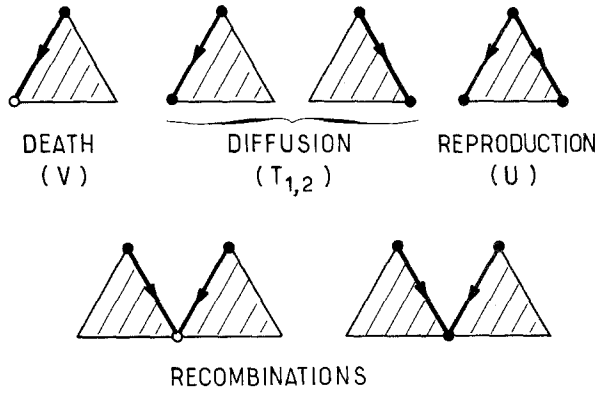

Fig. 9. Elementary diagrammatic processes encountered for correlation functions in the nonlinear case (1.2) when summing over one spin (first row) or two spins (second row).

2.5.1. How Large Is the Universality Class of Kinetic Ising Models?

It has been suggested[26] that *fully probabilistic* PCA which are *invariant under spin reverse* fall into the universality class of kinetic Ising models[34] (i.e., have the same critical behavior as those satisfying detailed balance). The argument is based on the hypothesis that the critical behavior of these PCA can be described by a Langevin equation:

$$\frac{\partial \phi}{\partial t} = Q_D[\phi] + \eta(t) \tag{2.43}$$

which is similar to (2.40), except for the fact that $Q_D[\phi]$ is no longer the derivative of a hamiltonian. Nevertheless, the authors of ref. 26 conclude that this modifies Q_D only by irrelevant terms in $D = 4 - \varepsilon$ space dimensions. This would mean, for example, that the critical behavior in Fig. 5c is the same at points F and AF as along the whole boundaries (except for the semideterministic linear endpoints). Note, however, that even if the critical phenomena have the same nature, other dynamical aspects (such as the growth of domain walls) may be—and are—quite different from the case where detailed balance is satisfied (see, e.g., ref. 49).

2.5.2. PCA in the Universality Class of Reggeon Field Theory. There are, however, examples in which new universality classes do appear. This is the case for our now familiar 1D PCA of Fig. 5b. In this case, a field-theoretic study can be performed, and phase transitions are found to be described by Reggeon field theory (RFT)[50] (except for the critical points of the linear case). This conclusion can be reached by

seemingly different methods or relations with other problems. We will briefly present them and point out that they are all different ways of seeing a unique problem. In doing so, the formulation of the PCA as a spin model and the diagrammatics above will be of great help.

Equivalence with Directed Percolation. As first shown by Domany and Kinzel,[10] when an absorbing state is present (i.e., on the sides $x=0$ or $z=1$ of the cubic phase diagram), these rules become equivalent to a mixed site-bond directed percolation problem[35] on the square lattice, defined as follows. Each site of the square lattice (viewed as in Fig. 1a) being present with a probability p and each bond with a probability q, one studies the propagation of an initially "wet" site, each bond "conducting water" only in the upward (diagonal) direction (the time direction in Fig. 1a) and provided both sites connected by the bond are present. Denoting a wet site by $S_{i,t}=+1$, the equivalence with the PCA of Fig. 5b is obtained, $P(1/S_{i-1,t},\ S_{i+1,t})$ being the probability that site $(i, t+1)$ is wet, knowing the state of $(i-1, t)$ and $(i+1, t)$. This requires that $x=P(1/-1,\ -1)=0$, since a site cannot be wetted by two dry neighbors, and leads to the following indentifications:

$$\begin{aligned} y &= P(1/-1,\ 1) = P(1/1,\ -1) = pq \\ z &= P(1/1,\ 1) = p[q^2 + 2q(1-q)] = pq(2-q) \end{aligned} \tag{2.44}$$

This equivalence suggests that we use here the method developed by Cardy and Sugar in their study of directed bond percolation (i.e., when $p=1$).[36] It starts from a direct operator representation of two-point correlation functions, which is obtained by implementing the diagrammatic rules of Fig. 9a. (Note that, as usual, these graphs are "directed" ones, with respect to the time direction.) A Gaussian transformation is performed, which introduces scalar fields $\phi(x, t)$ and $\bar{\phi}(x, t)$. Keeping only relevant terms in the continuous limit in $D=4-\varepsilon$ spatial dimensions leads to the RFT action for these fields, namely

$$S_{D+1} = \int dt\, dx^D \left[r_1 \bar{\phi}\, \partial_t \phi + r_2 \nabla_\perp \phi \nabla_\perp \bar{\phi} + m \bar{\phi} \phi + \frac{i}{2} (\bar{\phi}^2 \phi + \bar{\phi} \phi^2) \right] \tag{2.45}$$

It is straightforward that a value of p different from 1 induces only minimal changes in this analysis: thus, the directed-percolation phase transition on the sides $x=0$ (or $z=1$) of the phase diagram of Fig. 5b is in the universality class of RFT. The transition lines depicted have been determined numerically in ref. 10, and the values of the exponents $\nu_\perp$ and $\nu_{||}$ obtained

there agree with the result for RFT in $D=1$ (known from strong-coupling expansions[51]):

$$\nu_\perp = 1.105 \pm 0.005, \qquad \nu_{||} = 1.736 \pm 0.001 \tag{2.46}$$

The direction-dependent properties of this phase transition[31,52] are qualitatively the same as those described in Section 2.2 for the endpoint C (which is, however, in a different universality class). In particular, the characteristic velocity V_m vanishes at criticality as $V_m \sim |p - p_c|^{\nu_{||} - \nu_\perp}$. The question of the phase transitions for x, y, *and* z all different from 0 is not definitely settled; it is, however, likely that the equivalence with RFT also holds there (no qualitative change arises in the diagrammatics), but that no phase transition exists for these fully probabilistic rules, as is already the case at the mean-field level. (The above critical lines would thus separate two phases only when restricted to the side $x=0$ or $z=1$.) There is in fact a common belief that 1D PCA only have phase transitions when an absorbing site is present.

Equivalence with Schlögl's First Model and with a Quantum Spin Chain. The "reproduction" and "recombination" mechanisms involved in the diagrammatics of nonlinear PCA are reminiscent of Schlögl's models describing catalytic chemical reactions.[53] Indeed, the elementary processes of Fig. 9 mimic Schlögl's first model, which describes the evolution of a chemical species X diffusing in space and undergoing the following reactions:

$$\begin{aligned} X &\to 0 && \text{(death)} \\ X &\to 2X && \text{(reproduction)} \\ 2X &\to X \\ 2X &\to 0 \end{aligned} \qquad \left.\right\} \quad \text{(recombinations)} \tag{2.47}$$

[Notice in particular that the mean-field approach (2.10) is the one used in ref. 53 to study the phase transitions of this model.] This model is in fact the first stochastic process whose equivalence with RFT has been recognized.[54,55] This was done originally by relating the n-particle density of the model to the n-Pomeron amplitudes of RFT[54] or by constructing a quantum mechanical Hamiltonian[55] in a way similar to that of Appendix B. One then finds an equivalence with a quantum spin chain which is known independently to be a realization of RFT.[56]

A Reggeon Two-Dimensional Spin Model. It results from the above considerations that the 2D equilibrium spin model associated to the

PCA of Fig. 5b on the sides $x=0$ and $z=1$ belongs to the universality class of RFT. This provides us with an example in which the zero-temperature critical behavior at the intersection with the disorder variety is highly non-trivial. The constraint $x=0$ is a zero-temperature limit which restricts the space of spin configurations by excluding those with $(S_3, S_1, S_2)=(-1, +1, +1)$. With this restricted configuration space in mind, the coupling constants of the spin model on the triangular lattice read (Appendix A):

$$e^{8K_0}=\frac{z}{1-z}\left(\frac{1-y}{y}\right)^2$$

$$e^{8K_{13}}=e^{8K_{23}}=\frac{z}{1-z}, \qquad e^{8K_{12}}=\frac{z(1-z)}{[y(1-y)]^2} \tag{2.48}$$

$$e^{8h}=z^3(1-z)\left(\frac{y}{1-y}\right)^2 \qquad \text{(total magnetic field)}$$

In fact, the possibility of constructing a spin model belonging to the universality class of RFT was first pointed out by Cardy and Sugar[57] and model (2.48) does have some similarities with the one introduced there (while not obviously equivalent).

3. CONCLUSION AND PROSPECTS

We have been concerned in this paper with the general equivalence between a D-dimensional probabilistic cellular automata and a $(D+1)$-dimensional equilibrium spin model satisfying a "disorder condition." This equivalence consists in the identification of the probability measure over space-time histories of the PCA with the Boltzmann weight of an equilibrium spin model (the "disorder condition" on its coupling constants coming from the normalization of probability).

This appears as fruitful and interesting in two respects. First, it allows us to borrow techniques from the equilibrium statistical mechanics of spin models in order to study statistical properties of the dynamical behavior of PCA. Indeed, the associated equilibrium spin model provides a *global description* of the time developments of the PCA which is a useful tool both for intuitive reasoning and quantitative approaches. This has been our main concern throughout this paper. It allowed us to study the properties of remarkable classes of PCA such as "quasi-Hamiltonian" or "affine" ones. Diagrammatic methods have been introduced for the calculation of time-dependent correlation functions, which allow explicit calculations in some solvable cases and are in general useful guides, e.g., for analyzing phase

transitions of PCA through field-theoretic techniques. The second interesting aspect, which has only been indirectly dealt with in this paper, concerns the equilibrium statistical mechanics of spin models itself. Indeed, the "disorder variety" of a model (i.e., the subspace of the phase diagram under which the "disorder condition" between coupling constants is satisfied) appears as a remarkable subspace on which a spectacular decoupling arises. As a consequence, the exact expression of the partition function is known on this subspace, among other quantities. This is interesting not only from the point of view of exact results (these exact expressions can be used to check conjectures or to improve series expansions[58]), but also raises physical questions on these models. Indeed, we have seen on several examples that the critical behavior at the intersection of the disorder and critical varieties (which can be at zero or finite temperature) displays very peculiar features such as anisotropic scaling and critical exponents different from the generic exponents of the model, at variance with the usual irrelevance of anisotropy. Finding a general understanding of these points is still an active field of research. Also, possible experimental implications (such as correlation length anomalies; see Garel and Maillard[17]) should be kept in mind.

Let us conclude by pointing out two directions in which it seems to us that further investigations can and should be performed. We have already mentioned the first one, which is the understanding of critical phenomena. The techniques and results described in this paper are first steps in this direction. They could be good starting points for a systematic study of the universality classes, in particular through field-theoretic approaches. The second one is concerned with the deterministic limits of PCA. We have mentioned that their time developments correspond to ground states of the associated equilibrium spin model, as noticed in ref. 10. The zero-temperature limit is, however, taken in a peculiar way in order to remain on the disorder variety of the model. Despite this complication, it seems possible to use conventional techniques to study the nature of these ground states and of their first excitations (for some attempts in this direction, see ref. 45) in order to relate their properties (degeneracy, frustration, etc.) to the nature of the pattern of the automaton (complexity, etc.).

APPENDIX A

A.1. "Peripheral" PCA of Section 1.1.

In order to express the conditional probability $P(S_3/S_1, S_2)$ in exponential form, let us enumerate the $2^3 = 8$ spin configurations:

$$
\begin{aligned}
z &= \lambda^{-1} \exp(H_1 + H_2 + H_3 + K_{23} + K_{13} + K_{12} + K_0) \\
x &= \lambda^{-1} \exp(H_1 - H_2 - H_3 - K_{23} - K_{13} + K_{12} + K_0) \\
y_1 &= \lambda^{-1} \exp(-H_1 + H_2 - H_3 + K_{23} - K_{13} - K_{12} - K_0) \\
y_2 &= \lambda^{-1} \exp(H_1 - H_2 + H_3 - K_{23} + K_{13} - K_{12} - K_0) \\
1 - z &= \lambda^{-1} \exp(H_1 + H_2 - H_3 - K_{23} - K_{13} + K_{12} - K_0) \\
1 - x &= \lambda^{-1} \exp(-H_1 - H_2 - H_3 + K_{23} + K_{13} + K_{12} - K_0) \\
1 - y_1 &= \lambda^{-1} \exp(-H_1 + H_2 - H_3 - K_{23} + K_{13} - K_{12} + K_0) \\
1 - y_2 &= \lambda^{-1} \exp(H_1 - H_2 - H_3 + K_{23} - K_{13} - K_{12} + K_0)
\end{aligned}
\tag{A.1}
$$

The product of all these equations determines the normalization

$$
\lambda^{-8} = x(1-x)\, z(1-z) \prod_i y_i(1-y_i) \tag{A.2}
$$

As first noticed by Enting,[7] all coupling constants but one—L, for example—can be eliminated in Eq. (A.1) by taking the product of the four equations where L appears with a "plus" sign (this is due to the Z_2 symmetry). This leads to the desired expressions:

$$
\begin{aligned}
e^{8K_0} &= \frac{zx(1-y_1)(1-y_2)}{(1-z)(1-x)\, y_1\, y_2} \\
e^{8H_1} &= \frac{z(1-z)\, y_2(1-y_2)}{x(1-x)\, y_1(1-y_1)}, \qquad e^{8H_2} = (1 \leftrightarrow 2) \\
e^{8H_3} &= \frac{zxy_1\, y_2}{(1-z)(1-x)(1-y_1)(1-y_2)} \\
e^{8K_{23}} &= \frac{z(1-x)\, y_1(1-y_2)}{x(1-z)\, y_2(1-y_1)}, \qquad e^{8K_{13}} = (1 \leftrightarrow 2) \\
e^{8KL_{12}} &= \frac{zx(1-z)(1-x)}{y_1\, y_2(1-y_1)(1-y_2)}
\end{aligned}
\tag{A.3}
$$

Linear Case. The linear case is defined by $U = V = 0$: the 2D Hamiltonian thus becomes invariant by spin reverse, and one obtains the triangular zero-field Ising model on its disorder variety:

$$
\begin{aligned}
P(S_3/S_1, S_2)_{\text{linear}} &= 1/2[1 + S_3(T_1 S_2 + T_2 S_1)] \\
&= \lambda^{-1} \exp(K_{23} S_2 S_3 + K_{13} S_1 S_3 + K_{12} S_1 S_2)
\end{aligned}
\tag{A.4}
$$

In this case, the disorder condition simply reads

$$t_3 + t_1 t_2 = 0 \tag{A.5}$$

where we have set $t_i = \tanh(K_{jk})$. The T_i have the following expression in term of the K_{ij}:

$$\begin{aligned} T_1 &= t_1(1-t_2^2)/(1-t_1^2 t_2^2) \\ T_2 &= t_2(1-t_1^2)/(1-t_1^2 t_2^2) \end{aligned} \tag{A.6}$$

which can be easily inverted, using (A.3),

$$\begin{aligned} t_1 &= \frac{(1+T_1+T_2)^{1/2}(1+T_1-T_2)^{1/2} - (1-T_1-T_2)^{1/2}(1-T_1+T_2)^{1/2}}{(1+T_1+T_2)^{1/2}(1+T_1-T_2)^{1/2} + (1-T_1-T_2)^{1/2}(1-T_1+T_2)^{1/2}} \\ t_2 &= (1 \leftrightarrow 2) \\ t_3 &= \frac{[1-(T_1-T_2)^2]^{1/2} - [1-(T_1+T_2)^2]^{1/2}}{4T_1 T_2} \end{aligned} \tag{A.7}$$

A.2. General Case

Let us consider the 1D PCA of Section 1.3, together with the 2D one of Section 1.5. In nonexponential form, the conditional probability reads

$$\begin{aligned} P(S_3/S_1, S_0, S_2) = 1/2[1 + S_3(V + T_1 S_2 + T_2 S_1 + T_0 S_0 \\ + U_1 S_0 S_2 + U_0 S_1 S_2 + U_2 S_0 S_2 + W S_1 S_0 S_2)] \end{aligned} \tag{A.8}$$

with

$$\begin{aligned} V &= 1/4\left[x + z + \sum_i (y_i + v_i) - 4\right] \\ T_1 &= 1/4(z - x + y_2 + y_0 - y_1 + v_1 - v_2 - v_0), \ldots \\ U_1 &= 1/4(z + x + y_1 - y_0 - y_2 + v_1 - v_0 - v_2), \ldots \\ W &= 1/4\left[z - x + \sum_i (v_i - y_i)\right] \end{aligned} \tag{A.9}$$

Using the same method as for Eqs. (A.1), one can obtain P in exponential form as

$$\begin{aligned} &P(S_3/S_1, S_0, S_2) \\ &= \lambda^{-1} \exp\left(\sum_i H_i S_i + \sum_{ij} K_{ij} S_i S_j + \sum K_i S_j S_k S_l + L S_0 S_1 S_2 S_3\right) \end{aligned} \tag{A.10}$$

with

$$\lambda^{-16} = x(1-x)\, z(1-z) \prod_i y_i(1-y_i)\, v_i(1-v_i)$$

$$e^{16H_1} = \frac{z(1-z)\, y_0(1-y_0)\, y_2(1-y_2)\, v_1(1-v_1)}{x(1-x)\, v_0(1-v_0)\, v_2(1-v_2)\, y_1(1-y_1)}, \ldots$$

$$e^{16H_3} = \frac{xzy_1\, y_2\, y_3(1-v_1)(1-v_2)(1-v_3)}{(1-x)(1-z)(1-y_1)(1-y_2)(1-y_3)\, v_1 v_2 v_3}$$

$$e^{16K_{01}} = \frac{x(1-x)\, z(1-z)\, y_2(1-y_2)\, v_2(1-v_2)}{y_0(1-y_0)\, y_1(1-y_1)\, v_0(1-v_0)\, v_1(1-v_1)}, \ldots \tag{A.11}$$

$$e^{16K_{13}} = \frac{z(1-x)\, v_1(1-y_1)\, y_0(1-v_0)\, y_2(1-v_2)}{x(1-z)\, y_1(1-v_1)\, v_0(1-y_0)\, v_2(1-y_2)}, \ldots$$

$$e^{16K_1} = \frac{xzy_1 v_1(1-y_0)(1-v_0)(1-y_2)(1-v_2)}{(1-x)(1-z)(1-y_1)(1-v_1)\, y_0 v_0\, y_2 v_2}, \ldots$$

$$e^{16K_3} = \frac{z(1-z)\, v_0 v_1 v_2(1-v_0)(1-v_1)(1-v_2)}{x(1-x)\, y_0\, y_1\, y_2(1-y_0)(1-y_1)(1-y_2)}$$

$$e^{16L} = \frac{(1-x)\, zv_1 v_2 v_3(1-y_1)(1-y_2)(1-y_3)}{x(1-z)(1-v_1)(1-v_2)(1-v_3)\, y_1\, y_2\, y_3}$$

In the "peripheral" cases

$$x = v_0, \qquad z = y_0, \qquad y_1 = v_2, \qquad y_2 = v_1 \tag{A.12}$$

one can check that

$$H_0 = K_{01} = K_{02} = K_{03} = K_1 = K_2 = K_3 = L = 0 \tag{A.13}$$

and that the results (A.2)–(A.3) are recovered for the other coupling constants.

APPENDIX B. QUANTUM HAMILTONIAN DESCRIBING A PCA

One can associate a D-dimensional *quantum* Hamiltonian with a given PCA. Indeed, the probability $P[\{S_i\}; t]$ of a given configuration of the D-dimensional array of spins follows a master equation:

$$P[\{S_i'\}, t + \Delta t] = \sum_{\{S_i\}} p[\{S_i'\} \leftarrow \{S_i\}]\, P[\{S_i\}; t] \tag{B.1}$$

where p is the product of local conditional probabilities:

$$p[\{S_i'\} \leftarrow \{S_i\}] = \prod_i P(S_i' | \{S_j\}) \tag{B.2}$$

Defining the state $|\psi(t)\rangle$ of the system in such a way that $P[\{S\}; t] = \langle \{S\} | \psi(t) \rangle$, we have that $|\psi(t)\rangle$ follows a discrete-time Schrödinger equation with Hamiltonian H_Q given by

$$\langle \{S_i'\} | e^{-iH_Q \Delta t} | \{S_i\} \rangle = p[\{S_i'\} \leftarrow \{S_i\}] \tag{B.3}$$

Note that p is nothing but the row-to-row transfer matrix of the associated $(D+1)$-dimensional classical spin model; in this sense (B.3) simply expresses the well-known correspondence between a D-dimensional quantum spin model and a classical spin model in $D+1$ dimensions. It is, however, in general quite intricate to find an explicit expression of H_Q in terms of spin operators. This can be done, for example, in the case of Section 2.45 in order to establish the equivalence with Reggeon field theory.

APPENDIX C. QUASI-HAMILTONIAN RULES

In order to find the rule numbers which are deterministic limits of "quasi-Hamiltonian" PCA, it is convenient to cast condition (1.38) under the simpler form

$$\xi_1 \eta_1 = \xi_2 \eta_2 = \xi_0 \eta_0$$

$$\frac{\eta_1 \eta_2 \eta_0}{\xi_1 \xi_2 \xi_0} = \frac{x}{1-x} \frac{1-z}{z}$$

where the following variables have been introduced:

$$\xi_i = \frac{y_i}{1-y_i}, \qquad \eta_i = \frac{v_i}{1-v_i}$$

The problem is then to find the "points at infinity" of this eight-dimensional manifold. Let us give the complete list of the rule numbers found in this way, among the 256 deterministic rules of Section 1.3 (we only give the "minimal representing rule" numbers, which means that one has to add to this list all the transformed rules by conjugation and reflection): 0, 1, 2, 3, 4, 5, 7, 8, 10, 11, 12, 13, 14, 15, 19, 23, 27, 29, 32, 34, 35, 37, 42, 43, 50, 51, 58, 76, 77, 128, 136, 138, 140, 142, 160, 162, 164, 168, 170, 172, 178, 184, 200, 204, 232.

ACKNOWLEDGEMENTS

We are deeply indebted to J. M. Maillard for generously sharing his knowledge of exact results on spin models and of "disorder solutions." We thank him, together with D. Hansel, for a fruitful collaboration. We are grateful to J. P. Bouchaud for his careful reading of the manuscript. We thank P. Rujan for sending his preprint[12] while we were writing this work and for constructive criticisms. We also acknowledge discussions with M. Droz, and with J. Grinstein and J. Gubernatis during visits at IBM and CNLS (Los Alamos). Finally, we want to thank the referees for useful comments.

REFERENCES

1. W. Kinzel, *Z. Phys. B* **58**:29 (1985).
2. S. Wolfram, *Theory and Applications of Cellular Automata* (World Scientific, Singapore, 1986).
3. S. Wolfram, *Rev. Mod. Phys.* **55**:601 (1983); *Physica* **10D**:1 (1984).
4. J. Stephenson, *J. Math. Phys.* **11**:420 (1970); *Phys. Rev. B* **1**:4405 (1970); *Can. J. Phys.* **47**:2621 (1969).
5. T. R. Welberry and G. H. Miller, *Acta Cryst. A* **34**:120 (1978).
6. T. R. Welberry and R. Galbraith, *J. Appl. Cryst.* **6**:87 (1973); **8**:636 (1975); T. R. Welberry, *J. Appl. Cryst.* **10**:344 (1977).
7. I. G. Enting, *J. Phys. C, Solid State Phys.* **10**:1379 (1977).
8. P. Rujan, *J. Stat. Phys.* **29**:231, 247 (1982); **34**:615 (1984).
9. C. Bennet and G. Grinstein, *Phys. Rev. Lett.* **55**:657 (1985).
10. E. Domany and W. Kinzel, *Phys. Rev. Lett.* **53**:311 (1984).
11. E. Domany, *Phys. Rev. Lett.* **52**:871 (1984).
12. P. Rujan, Cellular automata and statistical mechanical models, IFK der KFA Jülich, *J. Stat. Phys.* **49**:139 (1987).
13. E. Domany and J. Gubernatis, *Phys. Rev. B* **32**:3354 (1985).
14. M. T. Jaekel and J. M. Maillard, *J. Phys. A Math. Gen.* **18**:1229 (1985).
15. A. M. W. Verhagen, *J. Stat. Phys.* **15**:219 (1976).
16. N. C. Chao and F. Y. Wu, *J. Phys. A Math. Gen.* **18**:L603 (1985).
17. I. G. Enting, *J. Phys. C Solid State Phys.* **6**:3457 (1973); T. Garel and J. M. Maillard, *J. Phys. C* **19**:L505 (1986).
18. J. M. Maillard, Lecture, Meeting on Random Schrödinger Equations, University of Arizona (February 1987); P. Rujan, in *Non-linear Equations in Classical and Quantum Field Theory*, N. Sanchez, ed. (Springer-Verlag, 1985), p. 286.
19. P. Bak, *Rep. Prog. Phys.* **45**:587 (1982); I. Peschel and V. J. Emery, *Z. Phys. B* **43**:241 (1981).
20. F. Y. Wu, *Rev. Mod. Phys.* **54**:235 (1982).
21. M. T. Jaekel and J. M. Maillard, *J. Phys. A Math. Gen.* **17**:2079 (1984); **18**:2271 (1985).
22. M. Y. Choi and B. A. Huberman, *J. Phys. A Math. Gen.* **17**:L765 (1984).
23. I. Peschel and T. T. Truong, *J. Stat. Phys.* **45**:233 (1986).
24. M. T. Jaekel and J. M. Maillard, *J. Phys. A Math. Gen.* **18**:641 (1985).
25. A. Georges, D. Hansel, P. Le Doussal, and J. M. Maillard, *J. Phys. A Math. Gen.* **20**:5299 (1987).
26. G. Grinstein, C. Jayaprakash, and Y. He, *Phys. Rev. Lett.* **55**:2527 (1985).

27. I. G. Enting, *J. Phys. A Math. Gen.* **11**:2001 (1978).
28. D. Dhar and J. M. Maillard, *J. Phys. A Math. Gen.* **18**:L383 (1985).
29. A. Georges, D. Hansel, P. Le Doussal, and J. M. Maillard, *J. Phys. A Math. Gen.* **19**:1001 (1986).
30. A. Georges, D. Hansel, P. Le Doussal, and J. M. Maillard, *J. Phys. A Math. Gen.* **19**:L329 (1986).
31. W. Kinzel, in *Percolation Structures and Processes*, G. Deutscher, R. Zallen, and J. Adler, eds. (Israel Physical Society, 1983).
32. B. K. Chakrabarti and S. S. Manna, *J. Phys. A Math. Gen.* **16**:L113 (1983).
33. J. Cardy, *J. Phys. A Math. Gen.* **16**:L355 (1983).
34. P. C. Hohenberg and B. I. Halperin, *Rev. Mod. Phys.* **49**:435 (1977).
35. S. P. Obukhov, *Physica* **101A**:145 (1980).
36. J. L. Cardy and R. L. Sugar, *J. Phys. A Math. Gen.* **13**:L423 (1980).
37. E. Domany and W. Kinzel, *Phys. Rev. Lett.* **47**:5 (1981).
38. S. W. J. Blöte and H. J. Hilhorst, *J. Phys. A Math. Gen.* **15**:L631 (1982).
39. S. M. Bhattacharjee, *Phys. Rev. Lett.* **53**:1161 (1984).
40. E. W. Montroll, in *Applied Combinatorial Mathematics*, E. F. Beckenbach, ed. (Wiley, New York, 1964).
41. S. M. Bhattacharjee, J. F. Nagle, D. A. Huse, and M. E. Fisher, *J. Stat. Phys.* **32**:361 (1983).
42. J. des Cloiseaux, *J. Phys.* **36**:281 (1975).
43. W. Feller, *An Introduction to Probability Theory and Its Applications*" (Wiley, New York, 1971), Vol. 1, p. 352.
44. A. Aharony, E. Domany, R. M. Hornreich, T. Schneider, and M. Zannetti, *Phys. Rev. B* **32**:3358 (1985).
45. G. Vichniac, *Physica* **10D**:96 (1984).
46. D. S. Zimmerman, C. Kalln, and A. J. Berlinsky, *Phys. Rev. Lett.* **58**:1881 (1987).
47. R. M. Hornreich, M. Luban, and S. Shtrikman, *Phys. Rev. Lett.* **35**:1678 (1975); D. Auerbach, Master Thesis, Weizmann Institute (1986).
48. G. Parisi and N. Sourlas, *Nucl. Phys. B* **206**:321 (1982).
49. J. Vinals and J. D. Gunton, *J. Phys. A Math. Gen.* **19**:L933 (1986).
50. H. Abarbanel, J. Bronzan, and A. Whote, *Phys. Rep.* **21**:119 (1975); M. Moshe, *Phys. Rep. C* **37**:255 (1978).
51. R. C. Brower, M. A. Furman, and H. Moshe, *Phys. Lett.* **76B**:213 (1978).
52. W. Klein and W. Kinzel, *J. Phys. A Math. Gen.* **14**:L405 (1981).
53. F. Schlögl, *Z. Phys.* **253**:147 (1972).
54. P. Grassberger and K. Sundermeyer, *Phys. Lett.* **77B**:220 (1978).
55. P. Grassberger and A. De La Torre, *Ann. Phys.* **122**:373 (1979).
56. R. C. Brower, M. A. Furman, and K. Subbarao, *Phys. Rev. D* **15**:1756 (1977).
57. J. L. Cardy and R. L. Sugar, *Phys. Rev. D* **12**:2514 (1975).
58. D. Hansel and J. M. Maillard, Preprint LPTHE 87/29, and references therein.
59. G. Vichniac, P. Tamayo, and H. Hartman, *J. Stat. Phys.* **45**:875 (1986).
60. B. Chopard and M. Droz, University of Geneva Preprint (1987).
61. Z. Racz, *Phys. Rev. Lett.* **55**:1707 (1985); J. Marro, J. L. Lebowitz, H. Spohn, and M. H. Kallos, *J. Stat. Phys.* **38**:725 (1985).
62. S. Katz, J. M. Lebowitz, and H. Spohn, *J. Stat. Phys.* **34**:497 (1984); J. S. Wang and J. L. Lebowitz, Phase transitions and universality in nonequilibrium steady states of stochastic Ising models, Preprint.
63. Liggett, *Interacting Particle Systems.*
64. T. Schneider, M. Zannetti, and R. Badii, *Phys. Rev. B* **31**:2941 (1985); T. Schneider and M. Schwatz, *Phys. Rev. B* **31**:7484 (1985).